

**LOW TEMPERATURE TESTING OF ONTARIO HOT MIX ASPHALT
AND RHEOLOGICAL TESTING OF RECOVERED BINDER**

by

BIDUR CHANDRA GHIMIRE

A thesis submitted to the Department of Chemistry

in conformity with the requirements for

the degree of Master of Science

Queen's University

Kingston, Ontario, Canada

(April, 2015)

Copyright © BIDUR CHANDRA GHIMIRE, 2015

Abstract

This thesis discusses and documents findings from an investigation of low temperature testing of asphalt mixes and rheological testing of binders. A number of asphalt mixes from the different Ontario Ministry of Transportation (MTO) and the City of Kingston construction contracts were investigated for their compliance with conventional Superpave® test methods such as indirect tensile test (IDT), dynamic shear rheometer (DSR) and bending beam rheometer (BBR) as well as additional specification tests such as extended BBR and double-edge-notched tension (DENT) test. To investigate the presence of polymer additives and waste engine oil in the binder X-ray fluorescence (XRF) and infrared spectroscopy (IR) tests were conducted. The American Association of State Highway and Transportation Official's Mechanistic-Empirical Pavement Design Guide (AASHTO MEPDG) software was used to predict long term low temperature performance of the mixtures in various regions of Ontario. The quality and durability of the binders recovered from some mixes were determined. Quality means the capacity of asphalt binder to reach a set of specific properties whereas durability is the measure of how well the asphalt resists change from its original characteristics when exposed to normal weathering and aging.

Tested contracts from the City of Kingston showed grade excesses when stored isothermally for three days at low temperatures according to Ontario's extended bending beam rheometer (BBR) protocol (LS-308) whereas most of the MTO contracts showed grade deficits. Few of the studied recovered asphalt samples showed deficient strain tolerance as measured in Ontario's double-edge-notched tension (DENT) test (LS-299).

The City of Kingston samples showed predicted times to failure from 9 to 15 years or greater whereas most MTO samples resulted in predicted times to failure of 1 to 5 years. X-ray

fluorescence and Fourier transform infrared spectroscopy (FTIR) indicated that most of the samples designed according to MTO specifications included waste engine oil and/or oxidized residues, both shown to reduce the performance of asphalt.

Acknowledgement

I would like to express my sincere thanks to my supervisor, Dr. Simon A. M. Hesp, for his kind support and guidance for the successful completion of my project. I am thankful to my supervisory committee members; Dr. Donal Macartney and Dr. Gary W. Vanloon, for their assistance towards a successful completion of my degree.

Special thanks go out to Phillip Maurer, who helped me to obtain and process IDT data. Thanks also goes out to Warren Lee of the Ontario Ministry of Transport for producing thermal cracking data using the AASHTO MEPDG software. I wish to thank Graeme Gillespie for his help with the collection of DENT data. I would also like to thank Professor H.F. Shurvell for his time and the Queen's Art Conservation Program for the use of their XRF equipment. I would also like to express thanks to my fellow lab mates; David Sowah-Kuma, John Omo Ikpugha and Isaac Omari for their help during my study period. I am equally grateful to the entire faculty, staff and students of the Department of Chemistry at Queen's University.

The Ministry of Transportation of Ontario (MTO) and the National Sciences and Engineering Research Council of Canada (NSERC) are acknowledged for their financial support towards this research.

Finally, I would like to give thanks to my parents, my wife Kanchan Devkota Ghimire and my daughter Prayusi Ghimire for their kind love, continuous support and encouragement.

Table of Contents

Abstract	ii
Acknowledgements.....	iv
Table of Contents	v
List of Figures	ix
List of Tables	xii
Abbreviations and Acronyms	xiii
Chapter 1 INTRODUCTION	1
1.1 Definition and Origin of Asphalt	1
1.2 Asphalt Concrete Pavement	2
1.3 Sources and Nature of Asphalt.....	3
1.4 Composition of Asphalt	4
1.5 Properties of Asphalt.....	6
1.5.1 Chemical Properties of Asphalt	6
1.5.2 Physical Properties of Asphalt	6
1.5.2.1 Durability	6
1.5.2.2 Adhesion and Cohesion	7
1.5.2.3 Temperature Susceptibility.....	7
1.5.2.4 Hardening and Aging.....	7
1.6 Asphalt Cement Performance Grade.....	7
1.7 Scope and Objectives	8

Chapter 2 BACKGROUND	10
2.1 Reversible and Physical Hardening of Asphalt.....	10
2.2 Superpave Mix Design.....	11
2.3 Failure Mode in Asphalt Cement.....	14
2.3.1 Fatigue Cracking.....	14
2.3.2 Rutting.....	16
2.3.3 Thermal Cracking.....	17
2.3.4 Moisture Damage.....	19
2.4 Viscoelastic Nature of Asphalt.....	20
2.5 Modification of Asphalt.....	23
2.5.1 Addition of Polymer.....	27
2.5.2 Polyphosphoric Acid (PPA) Addition.....	28
2.5.3 Air Blowing.....	29
2.6 Test Method Specifications.....	29
2.6.1 Conventional Methods.....	29
2.6.1.1 Penetration Test.....	29
2.6.1.2 Ring and Ball Softening Point Test.....	31
2.6.1.3 Viscosity Test.....	33
2.7 Superpave Specification Tests.....	33
2.7.1 Indirect Tensile (IDT) Creep and Strength Test.....	33
2.7.2 Dynamic Shear Rheometer Test.....	37
2.7.3 Bending Beam Rheometer Test.....	40
2.8 Improved Ministry of Transportation Ontario (MTO) Test Methods.....	42

2.8.1	Extended Bending Beam Rheometer Test LS-308.....	42
2.8.2	Double- Edge Notched Tension (DENT) Test LS-299.....	43
Chapter 3	MATERIALS AND EXPERIMENTAL.....	45
3.1	Materials.....	45
3.2	Experimental	46
3.2.1	Sample Preparation for IDT	46
3.2.1.1	Ageing	46
3.2.1.2	Mixing	47
3.2.1.3	Compaction	48
3.2.1.4	Cutting and Air Void Determination.....	48
3.2.2	Indirect Tensile Creep	49
3.2.3	Indirect Tensile (IDT) Strength.....	52
3.3	Extraction of Binder	53
3.4	Regular Bending Beam Rheometer Test [AASHTO M320]	53
3.5	Extended Bending Beam Rheometer Testing (MTO LS-308)	55
3.6	Dynamic Shear Rheometer (DSR) test	55
3.7	Double Edge Notch Tension (DENT) test	57
3.8	Fourier Transform Infrared Spectroscopy (FTIR)	58
3.9	X-Ray Fluorescence (XRF)	59
Chapter 4	RESULTS AND DISCUSSIONS.....	60
4.1	IDT Creep and Strength Testing	60
4.1.1	AASHTO MEPDG Software Results	67
4.2	Dynamic Shear Rheometer Analysis	69

4.2.1 High Temperature Superpave Grading	69
4.2.2 Intermediate Temperature Superpave Grading	70
4.2.3 Black Space Diagrams	71
4.3 Regular BBR Analysis	75
4.3.1 Low Temperature Grades	75
4.4 Extended BBR Analysis	77
4.4.1 Low Temperature Grades	77
4.5 Double Edge Notch Tension (DENT) Testing.....	78
4.5.1 Essential Works of Failure (We).....	80
4.5.2 Plastic Work of Failure	81
4.5.3 Approximate Critical Crack Tip Opening Displacements	82
4.6 XRF and FTIR Analysis of Recovered Asphalt	84
Chapter 5 SUMMARY, CONCLUSIONS AND RECOMMENDATIONS	88
REFERENCES.....	90

List of Figures

Figure 1.1: Basic flexible pavement structure [5].....	2
Figure 2.1: (a) Superpave gyratory compactor [23].....	13
Figure 2.1: (b) SGC mold configuration and compaction parameters [23]	13
Figure 2.2: Alligator cracking [29]	15
Figure 2.3: Rutting on wheel path [28].....	17
Figure 2.4: Thermal cracking [37].....	18
Figure 2.5: Moisture damage [8]	20
Figure 2.6: Mechanical response of elastic, viscous and viscoelastic materials under constant stress [41].....	22
Figure 2.7: (a) Sol-type Asphalt [44].....	24
Figure 2.7: (b) Gel-type Asphalt [44]	24
Figure 2.8: Penetration test equipment [58].....	30
Figure 2.9: Softening point test set up [15].....	32
Figure 2.10: Dynamic Shear Rheometer.....	39
Figure 2.11: Bending Beam Rheometer [15].....	41
Figure 3.1: Bucket Mixer	47
Figure 3.2: Pine Instruments AFG 2 Superpave™ gyratory compactor.....	48
Figure 3.3: Struers Automated Cutting Saw	49
Figure 3.4: Sample Loading Fixture and Test Frame	50
Figure 3.5: (a) Deflected Asphalt Beam on Bending Beam Test [75]	54
Figure 3.5: (b) Creep stiffness of asphalt binders based on change in deflection with time.....	54

Figure 3.5: (c) Evaluation of m-value of asphalt binders.....	55
Figure 3.6: DSR sample (A) and Spindles (B) [15].....	56
Figure 3.7: DENT sample preparation [27]	58
Figure 4.1: Creep Compliance curve at different temperatures	60
Figure 4.2: Creep compliance master curves for tested samples	61
Figure 4.3: Creep compliance master curves Hwy 28 and JCB	62
Figure 4.4: Comparison of creep compliance master curve after 3 and 72 h ageing for JCB -4% air voids.....	63
Figure 4.5: Comparison of creep compliance master curve after 3 and 72 h ageing for JCB -6% air voids.....	64
Figure 4.6: Comparison of creep compliance master curve after 3 and 72 h ageing for Hwy 28.	64
Figure 4.7: Strength values @-10 and -20 for tested samples.....	65
Figure 4.8: Tensile strength for Hwy 28 and JCB after 3 and 72 h conditioning.....	66
Figure 4.9: MEPDG results showing total length of thermal cracking for tested samples over time.....	68
Figure 4.10: Limiting high temperature grades of recovered asphalts	69
Figure 4.11: Limiting temperature of intermediate temperature grade of recovered asphalt	70
Figure 4.12: (a) – (g) Black space diagram.....	72
Figure 4.13: Low temperature grades of recovered binders.....	76
Figure 4.14: Low temperature grades of recovered binders extended BBR.....	77

Figure 4.15: (a) Representative Force-Displacement Data for the DENT Test for Burbrook	79
.....	
Figure 4.15: (b) Representative Force-Displacement Data for the DENT Test for Hwy	
401-1.....	80
Figure 4.16: Essential work of fracture for recovered binders from different contracts.....	81
Figure 4.17: Plastic work of failure for recovered binders from different contracts.....	82
Figure 4.18: CTOD values for all recovered binders.....	83
Figure 4.19: Zinc and molybdenum content of all samples, relative to Newalta waste engine oil	
residue sample.....	85
Figure 4.20: Carbonyl, butadiene, and styrene content of all samples, normalized to CH stretch	
peak area.....	87

List of Tables

Table 1.1: Methods Used to Produce and Process Asphalt	4
Table 2.1: Asphalt Modifier Type	26
Table 3.1: Sample contracts	45
Table 3.2: Ageing of different sample contracts.....	46
Table 4.1: Summary of MEPDG thermal cracking results	67
Table 4.2: BBR summary of recovered binders.....	78
Table 4.3: Table 4.3: Relative zinc and molybdenum counts obtained from XRF analysis.....	84
Table 4.4: Relative amounts of carbonyl, butadiene, and styrene obtained from FTIR analysis.....	86

Abbreviations and Acronyms

AASHTO	American Association of State and Highway Transportation Officials
APP	Atactic Polypropylene
ASTM	American Society for Testing and Materials
BBR	Bending Beam Rheometer
BSG	Bulk Specific Gravity
CTOD	Critical Crack Tip Opening Displacement
CoV	Coefficient of Variation
DENT	Double-Edge-Notched Tension
DSR	Dynamic Shear Rheometer
EA	Ethylene Acrylate
EBA	Ethylene Butyl Acrylate
eBBR	Extended Bending Beam Rheometer
EPDM	Ethylene Propylene Diene Terpolymer
EVA	Ethylene Vinyl Acetate
EWf	Essential Work of Fracture
FTIR	Fourier Transform Infrared
GL	Gauge Length
GPa	Giga Pascal
HMA	Hot Mix Asphalt
IDT	Indirect Tension Tests
JCB	John Counter Boulevard
kPa	Kilo Pascal

keV	Kilo Electrovolt
LDPE	Low Density Polyethylene
LVR	Linear Viscoelastic Range
MEPDG	Mechanistic-Empirical Pavement Design Guide
mN	Mili Newton
MTO	Ministry of Transportation of Ontario
MTS	Material Testing System
NHCRP	National Cooperative Highway Research Programme
PAV	Pressure Aging Vessel
PBD	Polybutadiene
PE	Polyethylene
PET	Polyethylene Terephthalate
PG	Performance Grade
PI	Penetration Index
PMA	Polymer Modified Asphalt
PP	Polypropylene
PPA	Polyphosphoric Acid
PVC	Polyvinyl Chloride
RTFO	Rolling Thin Film Oven
SB	Styrene Butadiene
SBR	Styrene Butadiene Rubber
SBS	Styrene Butadiene Styrene
SEBS	Styrene Ethylene Butadiene Styrene

SGC	Superpave Gyrotory Compactor
TFOT	Thin Film Oven Test
TLA	Trinidad Lake Asphalt
VFA	Voids Filled With Asphalt
VMA	Voids in Mineral Aggregate
WMA	Warm Mix Additives
XRF	X-Ray Fluorescence

Symbols

A	Temperature Susceptibility Parameter
a	Length of a sharp crack, m
b	Beam width, 12.5mm
B	Specimen Thickness, m
G*	Complex shear modulus, Pa
G'	Storage modulus, Pa
G''	Loss modulus, Pa
h	BBR beam thickness, 6.25 mm
K	Stress intensity factor, N
L	Ligament length, mm
%	Percent
P	Peak Load, N
D	Specimen diameter, mm
H	Specimen height, mm
T	Specimen thickness, mm
π	pi (3.142)

Chapter 1

INTRODUCTION

1.1 Definition and Origin of Asphalt

Asphalt has a different name and state according to the application, origin and from where it is obtained. It varies from being a solid to semi-solid at normal temperatures. In Europe, asphalt cement is commonly known as bitumen. It is normally a sticky, black and highly viscous liquid or semi-solid form of petroleum residue. It may be found in natural deposits or may be a refined product. Until the 20th century, the term asphaltum was also used [1]. The major use of asphalt is in road construction, where it is used as a binder mixed with aggregate particles to create asphalt concrete. The other main uses for asphalt are for waterproofing products, including the production of roofing felt and for the sealing of flat roofs [2].

The terms *asphalt* and *bitumen* are frequently used interchangeably, which means both represent natural and manufactured forms of the substance. In American English, asphalt (or asphalt cement) is the refined residue from the distillation process of selected crude oils. Outside of the United States, the product is often called bitumen. According to the American Society for Testing and Materials (ASTM 1998), asphalt cement is defined as a “*dark brown or black cementitious material occurring in nature or obtained by crude oil refining where the predominate material is mainly bitumen*” [3]. The term *bitumen* is preferred for geological language. Common usage often denotes to various forms of asphalt/bitumen as “tar”, such as at the La Brea Tar Pits. Another term “pitch” was preferred for asphalt in ancient time.

1.2 Asphalt Concrete Pavement

Because of the mixing and compaction at high temperatures during construction, asphalt concrete pavement is commonly known as hot mix asphalt (HMA) pavement. Asphalt concrete is a mixture of coarse aggregates, fine aggregates and asphalt binders. Generally, asphalt mixes are produced by heating the asphalt cement to about 160°C and blending it at about 5 weight percent with aggregate. Normally, HMA is applied in 5-10 cm thick layers with the lower part of the pavement supporting the top layer which is known as the surface or friction course. The function of the aggregates in the lower layer is to prevent rutting and fatigue cracking, while the aggregates in the surface course are responsible for their friction properties and durability [4].

A pavement's structure consists of three main components: the foundation, the base and the surface layer. All the components are responsible for the overall performance of a pavement. The foundation is made up of the sub-grade or the sub-base. The foundation carries the loads produced by construction traffic. Generally road pavements are of two types: rigid pavements and flexible pavements.



Figure 1.1: Basic flexible pavement structure [5].

1.3 Sources and Nature of Asphalt

Two main sources of asphalt are natural asphalt and petroleum asphalt.

Natural Asphalt: It is obtained from nature and found in “asphalt lakes” around the world. Natural deposits of asphalt comprise lakes such as the “Pitch Lake” in Trinidad and Tobago and “Lake Bermudez” in Venezuela. About 2.7×10^{12} barrels of asphalt including tar sands has been estimated to exist in various locations around the world. In Canada, about 95% of natural asphalt cement is found in the oil sands regions of Alberta. Northern Alberta contains a large deposit around the Athabasca region [6].

Petroleum Asphalt: Asphalt obtained during the refinery process of heavy crude oils is called petroleum asphalt. It is also defined as that part of a crude oil which is separated from the higher-boiling crude hydrocarbons oil upon the addition of lower-boiling hydrocarbon solvents such as propane, pentane, hexane or heptane, leading to precipitation. The precipitated material consists of asphaltenes which have an average molecular weight of about 800 - 2500 g/mole and exist in the form of flat sheets of polyaromatic condensed rings with short aliphatic chains [7]. Nowadays the asphalt produced through the refinery of crude oil is mostly used in North America. The methods used to produce and process asphalt materials are shown in Table 1.1.

Table 1.1: Methods Used to Produce and Process Asphalt [8].

Production/Process	Base Material	Product
Atmospheric and Vacuum Distillation	Asphalt-based Crude or Crude Mix	Asphalt Cements
Blending	Hard and Soft Asphalt Asphalt Cements and Petroleum Distillates	Asphalt Cements of Intermediate Consistency Cutback Asphalts
Air-Blowing	Asphalt Flux	Asphalt Cements, Roofing Asphalt, Pipe Coating, Special Membranes
Solvent Deasphalting	Vacuum Residuum	Hard Asphalt
Solvent Extraction	Vacuum Residuum	Asphalt Components (Asphaltenes, Resin, Oils)
Emulsification	Asphalt, Emulsifying Agent, and Water	Emulsified Asphalts
Modification	Asphalt and Modifiers (Polymers, Chemicals, etc.)	Modified Asphalts

1.4 Composition of Asphalt

Asphalt is made from crude petroleum, a naturally formed product from organic matter originating from plants that lived more than a million years ago under different conditions of temperature and pressure. About 90 to 95 percent by weight of asphalt is made up of carbon and hydrogen. The remaining parts contain metals and heteroatoms. Mostly, the heteroatoms such as nitrogen, oxygen and sulfur are present in the asphaltene fraction and contribute to the unique physical and chemical properties of asphalt [9].

Metal atoms such as vanadium, nickel and iron are present in very small quantities of less than one percent. These metals act as fingerprints which enable us to identify the source of an asphalt

cement. Solubility of different molecules in different solvents can be used to separate and evaluate the asphalt components. Two commonly used fractionation methods are Corbett chromatography and Rostler method. Corbett chromatographic method uses solubility of asphalt in suitable solvent and Rostler method uses precipitation technique [9].

Basically, there are three types of molecules: aliphatic, cyclic and aromatics. The aliphatic molecules are linear, three-dimensional chain-like molecules that are oily and waxy in nature. Cyclic molecules are called naphthenic which are three-dimensional saturated rings of carbon atoms with various atoms attached. Weak chemical bonds that hold the asphalt molecules together are easily broken by heat and shear stress. This explains the viscoelastic nature of asphalt. When asphalt is heated, the intermolecular bonds are broken and it flows freely. When the asphalt cools, weak intermolecular bonds reform and chemical structure returns [9]. All of the molecules in asphalt can be categorized in types: polar and non-polar. The polar components are responsible for elastic properties whereas nonpolar components are responsible for viscous properties.

Chemical composition of asphalt is very complex. However, it is possible to classify asphalt into two broad chemical groups called asphaltenes and maltenes. Maltenes can further be classified into saturates, aromatics and resins. Saturated compounds consist of straight and branched chain aliphatic hydrocarbons together with alkyl-naphthalenes and some alkyl aromatics 5 to 20% asphalt contain saturated part. Aromatic includes the lowest molecular weight naphthenic aromatic compounds in the asphalt. They set up 40 to 60% of total asphalt. Resins are largely composed of hydrogen and carbon and contain small amount of oxygen, sulphur and nitrogen [10].

1.5 Properties of Asphalt

1.5.1 Chemical Properties of Asphalt

The behavior of asphalt can be predicted from a basic knowledge of its chemistry, although asphalt cements for hot-mix asphalt pavements are hardly characterized by their chemical composition [3]. When asphalt is dissolved in a solvent such as n-heptane, it can be separated into two major parts: asphaltenes and maltenes. The asphaltene part is responsible for the colour and hardness of asphalt. The maltene part is soluble in heptane. A number of factors, such as high temperature, exposure to oxygen and light, type of aggregate used in pavement mixture, and the thickness of the asphalt film on aggregate particles, are responsible for changing the proportion of maltenes and asphaltenes in asphalt. The changes that happen include evaporation of more volatile components, oxidation, polymerization and other chemical reactions that can considerably influence the properties of asphalt [11].

1.5.2 Physical Properties of Asphalt

The important properties of asphalt comprise durability, adhesion, temperature susceptibility, hardening and aging [11, 12].

1.5.2.1 Durability

Durability can be defined as the measure of the ability of the asphalt to maintain satisfactory rheology, cohesion and adhesion in long-term service. This property depends on the pavement performance, not only on the asphalt alone. The property is tested by Thin Film Oven Test (TFOT) and Rolling Thin Film Oven Test [11].

1.5.2.2 Adhesion and Cohesion

Adhesion is the ability of asphalt to stick to the aggregate in the paving mixture. Cohesion is the ability of asphalt to hold the aggregate particles firmly in place in the finished pavement. The cohesive strength of asphalt is characterised by its ductility at low temperature [10].

1.5.2.3 Temperature susceptibility

Temperature susceptibility plays a great role in physical properties of asphalt. Asphalts become harder as their temperature decreases and becomes softer on increasing temperature. Temperature susceptibility depends on the petroleum source of asphalt, whatever the performance grade.

1.5.2.4 Hardening and Aging

Hardening of asphalt can play a major role in thermal cracking of flexible pavements. Oxidation is the primary cause of hardening of asphalt. The increase in stiffness and the decrease in the ability to relax stress due to hardening can cause the build-up of shrinkage stress in asphalt mixtures leading to a premature failure of pavement [13].

1.6 Asphalt Cement Performance Grade

Performance Graded (PG) binders are commonly known by their asphalt cement performance grade. The selection of performance graded binders depend on the climate and traffic at location where it will be used. An example of a PG binder designation is PG 64-22. The first number 64 is the high temperature in degree Celsius that the pavement is likely to reach. The second number -

22 is the lowest service temperature expected over a fifty year period. PG 64-22 asphalt is soft enough to resist low temperature thermal cracking down to a temperature of -22 degree Celsius. The high number 64 is the highest temperature up to which asphalt will be stiff enough to prevent a pavement from rutting due to traffic during a very hot week in summer. Polymer or other chemicals as modifier can be used to reduce temperature susceptibility and age hardening, resistance to low temperature cracking and improvement of stiffness of asphalt at high temperature [9, 14]. Cost of modified asphalt is nearly twice as much as unmodified asphalt. The current specification sets a limit on creep stiffness and the slope of the creep stiffness master curve to limit damage at the pavement design temperature [9].

Due to lack of enough chemical knowledge to explain asphalt properties, generally physical or mechanical testing methods are used to evaluate their performance. So, different methods are developed to classify asphalts to know their properties and predict their performance by conventional testing methods and more recently, Superpave™ methods [15].

1.7 Scope and Objectives

Many roads built in Ontario fail early. Low temperature cracking is one of the main distresses on asphalt pavements in Ontario. In fact, large amounts of money are spent annually to repair roads. In order to reduce rehabilitation costs and ensure the lowest possible impact on users, it is important to understand the actual cause of premature failures and to use corrective techniques to minimize future failures. To construct a better quality road, pavement design specifications need to be revised.

The aim of this study was to measure mechanical properties and compare the predicted performance of highway sample mixes designed by the Ontario Ministry of Transportation (MTO) to samples designed using specifications developed for the City of Kingston. The analysis was done using the American Association of State Highway and Transportation Officials' (AASHTO) mechanistic-empirical pavement design guide (MEPDG) and the AASHTO Pavement ME design software which uses low temperature creep and strength test input data from laboratory indirect tension tests (IDT). Prediction of the expected performance of roads, based on physical properties obtained from testing, weather and traffic data was done with the help of MEPDG. In addition to this, the high and low temperature performance grades, rheological properties, and failure properties of recovered binders were also determined. The properties were measured by regular tests (BBR and DSR) and modified new test such as extended BBR test (MTO method LS-308) and DENT test (MTO method LS-299).

In this study, indirect tensile (IDT) creep and IDT strength test results used for cracking prediction are included. Furthermore, the effect of long time aging at low temperature on sample performance is presented. Finally, the data obtained from Fourier transform infrared (FTIR) spectroscopy as well as X-ray fluorescence (XRF) are used to propose the probable explanation for the discrepancy between MTO and City of Kingston samples.

Chapter 2

BACKGROUND

2.1 Reversible and Physical Hardening of Asphalt

Physical hardening is a reversible process that could influence the long-term performance of a material and takes place below room temperature. It can be attributed to the restructuring of asphalt molecules to approach an ideal thermodynamic state under a specific set of conditions. Despite increased interest in this area, physical hardening remains one of the least understood physio-chemical phenomena affecting physical and rheological properties of asphalt [16, 17]. During cooling and storage at a constant low temperature, the stiffness of a binder increases and physical hardening takes place. The effect of physical hardening is completely removed when the asphalt binder is heated to room temperature or above. Physical hardening in polymers was first reported by Struik [18] and it was later introduced in asphalt binders during the Strategic Highway Research Program (SHRP), i.e. a recent investigation of the rheological properties of paving grade of asphalt cement. Physical hardening is similar to physical aging for many amorphous solids such as polymers [18, 19].

At ambient temperature, physical hardening of bitumen is a slow process that can continue for days, months and even years [17]. The low-temperature hardening rate is decreased quickly with time and depends on bitumen type at temperature close to and below the glass transition temperature [20, 21]. The hardening process is considered to be a slow isothermal sol-gel transformation. The phenomenon was described by the term ‘steric hardening’ by Brown et al. in the 1950s [22].

Physical hardening may be due to the reorganization of bitumen microstructural systems to approach an ideal thermodynamic state under a specific set of conditions. The process includes breaking and restructuring weak bonds in bitumen. Generally, the rate of physical hardening is quicker at the beginning, but decreases with increasing storage time at constant temperature [17]. When the temperature of asphalt cement is decreased from high temperature, its volume decreases due to a reduction in free volume and finally it reaches equilibrium. Once the glass transition region is reached, the molecular transport mobility is reduced and achieves in non-equilibrium volumes. In this case, the asphalt is in a metastable state which causes the material to constantly shrink isothermally. More closely packed molecular arrangement and reduced molecular mobility is obtained due to the decrease in free volume. The viscoelastic properties change with time and the material hardens. The physical hardening is time dependent and it depends on the temperature. The lower the temperature, the higher the hardening phenomenon and hardening rate. The hardening rate also depends on the chemical composition of the asphalt binder such as length of molecular chains, wax content, etc. [18, 19].

2.2 Superpave Mix Design

The aim of a mix design is to determine the best mixture of component materials required for the performance of the pavement. In asphalt mixture, binder and aggregate are mixed together in exact proportions. The comparative proportions of these materials determine the physical properties of the asphalt mixture and finally how the asphalt mixture performs as a finished pavement. One of the mix design methods is known as Superpave and it also determines the suitable proportions of asphalt binder and aggregate in the mixture. The Superpave mix design method is a volumetric mix design process. In this process, the evaluation of properties like voids in mineral aggregate

(VMA), voids filled with asphalt (VFA), air voids, and the dust/ effective binder ratio is determined by an analysis of specimens and the maximum specific gravity of the sample. This information is used to determine the parameters that require adjustment before making additional specimens. To produce the samples with desired volumetric properties with designed aggregate structure and the binder content the above process is repeated several times. The Superpave mix design consist of three basic steps [23].

Aggregate selection: Aggregate is specified in three ways. First, specification of aggregate gradation. Second, requirements of physical property of aggregate like angularity, flat and soundness.

Asphalt binder selection: Selection of the Superpave PG binders are based on the expected pavement temperature extremes in the area of their future use.

Optimum asphalt binder content determination: In Superpave method, this step is further divided in to four sub steps.

- Preparation of several initial samples: Usually, two samples are prepared at the proposed design asphalt content, two at 0.5% below designed asphalt content and two at 0.5% above designed asphalt content.
- Compaction of trial mixes in Superpave Gyrotory Compactor: The gyrotory simulates the mix densities obtained under the actual pavement climate and loading condition. The internal angle of gyration of SGC is required to be $1.16 \pm 0.02^\circ$. The analysis of specimens compacted with the Superpave gyrotory compactor is done at a different number of gyrations depending on the traffic for the contract and whether the mixture is dense graded,

open graded, or a stone mastic asphalt (SMA) mixture [24]. The pictorial representation of SGC is shown in Figure 2.1(a) and (b).

- Determination of density and other volumetric properties of samples.
- Selection of optimum binder content corresponding to 4% air voids.

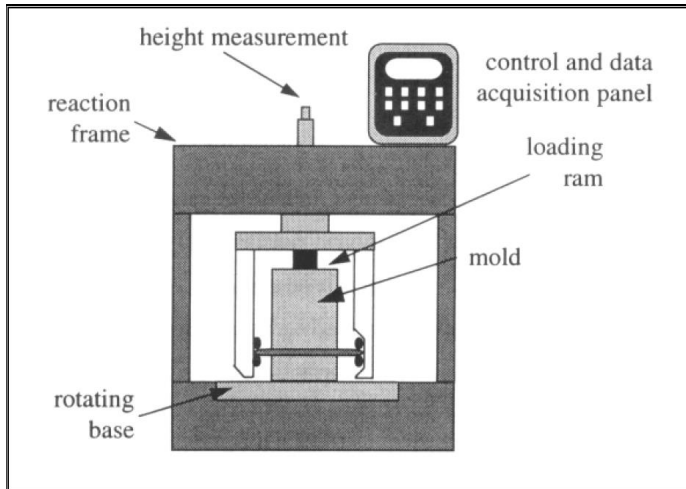


Fig 2.1(a): Superpave gyratory compactor [23].

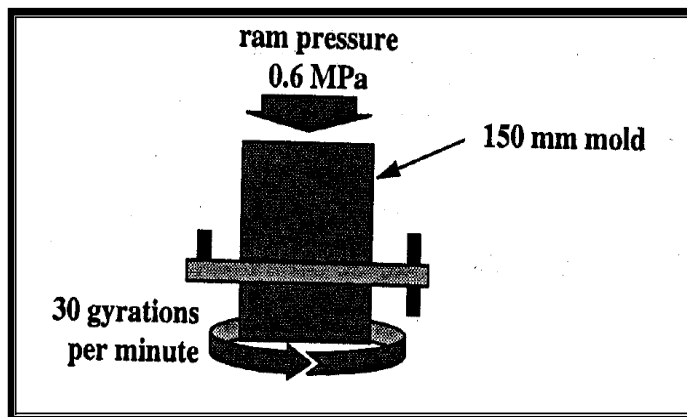


Fig 2.1(b): SGC mold configuration and compaction parameters [23].

2.3 Failure Modes in Asphalt Pavements

The failure modes in asphalt is also known as distresses in asphalt. Several factors such as rain, sunlight, oxygen, chemicals, thermal stresses, distortions, and disintegrations, with the application of traffic load repetitions over a period of time are the causes of failure of asphalt pavement through rutting, fatigue cracking, low temperature cracking, and moisture damage. Generally, in all weather conditions, the asphalt used in a pavement must remain visco-elastic but this does not happen practically. Mainly, two factors are responsible for the failure modes in asphalt: environmental and structural. Environmental factor is due to weathering and aging and structural caused by repeated traffic loadings. The rate at which pavement distresses appear depends on its environment, traffic loading conditions, original construction quality and temporary maintenance procedures. The life of the pavement can significantly be reduced by poor quality materials or poor construction procedures. Consequently, two pavements built at the same time may have considerably different life cycles or certain portions of a pavement may worsen more rapidly than others. Therefore, timely and effective maintenance can increase a pavement's life. Crack sealing and seal coating can reduce the effect of moisture in aging of asphalt pavement [14]. During summer, all asphalts become soft and form ruts or permanently deform. During winters, arrangement of neutral molecules in the asphalt takes place into more organized structural forms, which in turn harden the material leading to brittleness and the formation of cracks under high traffic loads. These processes are termed as fatigue and thermal cracking [25].

2.3.1 Fatigue Cracking

When repeated loading by vehicles under moderate and low temperature conditions is applied on pavement and induces stress that is more than the fatigue limit of the pavement then fatigue

cracking occurs. It is also known as alligator cracking since its pattern resembles the skin of an alligator. In thin pavements, cracking initiates at the bottom of the HMA layer where the tensile stress is the highest then propagates to the surface. This is commonly represented as bottom-up or classical fatigue cracking. In thick pavements, the cracks generally initiate from the top of the pavement where high tensile stresses resulting from tire-pavement interaction and asphalt binder aging. After repeated loading, the longitudinal cracks join forming many-sided sharp-angled pieces that develop into a pattern resembling the back of an alligator or crocodile [26]. Potholes develop in fatigue cracking by the action of traffic loads which separate the pavement surface from the underlying layers [27]. Several factors like environment and climatic condition, pavement structure, mixture composition and construction are responsible for fatigue cracking [28]. This can be characterized by loss modulus obtained from dynamic shear rheometer (DSR) test and even better by the use of the double-edge notched tension (DENT) test.



Figure 2.2: Alligator cracking [29].

2.3.2 Rutting

Rutting is the accumulation of permanent deformation in the paving layers. It is caused by a combination of densification and shear deformation, appearing as longitudinal depressions in the wheel paths and small upheavals to the sides [30-31]. Rutting has a substantial effect on the performance of asphalt pavement, in particular the ruts trap water to cause hydroplaning [30-32]. Furthermore, significant rutting can be the cause of major structural failures [30-33]. Hence, the rutting not only reduces service life, but it may also affect the safety of highway users. It is necessary to investigate the causes that lead to rutting in asphalt pavements. Rutting typically occurs at high temperatures by unrecoverable strain accumulated from repeated loads to the asphalt pavement. Heavy loads at low frequencies or high temperatures are the major causes of this failure. Rutting mainly occurs under hot climatic conditions where the asphalt binder viscosity is decreased and flow can occur under traffic loading. Eventually, the formation of ruts or tracks in the asphalt surface layers takes place [33]. It is well known that variations in material properties are a major factor to influence the rutting resistance of asphalt mixtures [30-34]. Many researchers have conducted a lot of work on it [33]. Simultaneously, different test methods were utilized to estimate the rutting performance of asphalt pavement. In current years, visco-elasticity theory, especially linear visco-elasticity models, have been developed to predict the rutting in asphalt pavements [30-35]. Basically, there are two types of rutting: mix rutting and subgrade rutting. Due to improper compaction or mix design problems the pavement surface exhibits wheel path depressions but subgrade does not rut yet, such distress is called mix rutting. Occurring of subgrade rutting takes place when the subgrade exhibits wheel path depressions due to loading. In this situation, the pavement settles into the subgrade ruts causing surface depressions in the wheel path [28]. The

rutting resistance factor, $G^*/\sin\delta$ (where G^* is the complex modulus and δ is the phase angle) helps to predict the rutting behavior and it can be measured by using a dynamic shear rheometer (DSR).



Figure 2.3: Rutting on wheel path [28].

2.3.3 Thermal Cracking

Low temperature cracking is the most widespread distress found in asphalt pavements constructed in cold weather climates. Low temperature cracking is the main cause of pavement roughness and reduced service life in northern climates. The restrained pavement tries to shrink when the temperature drops. The tensile stresses build up to a critical point at which a crack is formed. Thermal cracks can be initiated by a single low temperature event or by multiple freeze and thaw cycles and then propagated by further low temperatures or traffic loadings [36]. Thermal cracking is a major form of road pavement failure in Canada and the northern United states. It occurs as a result of three different processes [37].

- The immediate drop in temperature below the certain limit build up the stress above the strength of the mix. This is called single-event thermal cracking.
- The repetitive thermal stress below the critical value reduces the strength of asphalt mix and causes the failure of pavement, even though the expected critical stress was not achieved. This is referred as thermal fatigue cracking.
- Additional transverse cracking can be observed due to the impact of recurrent loading by regular vehicles, heavy truck traffic and freeze-thaw cycles. This is called mixed load or thermal distress cracking.



Figure 2.4: Thermal cracking [37].

2.3.4 Moisture Damage

Moisture damage is defined as the deterioration of asphalt pavement due to loss of adhesion between asphalt binder and aggregate surface or loss of cohesion within the binder due to water [38]. The liquid asphalt binder holds the pavement together and acts as waterproof material of the pavement. When moisture gets to the surface of the aggregate it can break the asphalt - aggregate bond, causing the pavement to disintegrate [39]. Moisture damage is due to stripping (breaking the adhesive bond between asphalt binder and aggregates surface) and/or softening (reduction of asphalt concrete cohesion). Basically following factors are responsible for stripping [39]:

- Poor asphalt/aggregate bond;
- Improper compaction;
- Excess dust;
- Clay/deleterious fines;
- Lean mixes;
- Poor drainage; and
- Cracks allowing moisture intrusion.

Moisture damage can be prevented by applying the following:

- Proper compaction;
- Proper drainage;
- Aggregate with rough surface;
- Anti-stripping agent; and

- Good quality asphalt binder.



Figure 2.5: Moisture damage [8]

2.4 Viscoelastic Nature of Asphalt

Asphalt binder is a viscoelastic materials since it shows both elastic and viscous characteristics at the same time. Viscoelastic behaviour of asphalt cement depends on temperature and loading time. At high temperature (above 100°C), asphalt binder behaves almost like as viscous liquid. It acts mostly like an elastic solid, recovering to its original shape when on applying load and removing load at very low temperature (below 0°C). At intermediate temperatures it has characteristics of both a viscous liquid and elastic solid [40]. Asphalt binder deforms when load is applied. Both elastic response and viscous flow are responsible for deformation.

The characteristic response of elastic, viscous and viscoelastic materials with applied stress is shown in Figure 2.6. An elastic material experiences recoverable deformation on applying constant (or creep) load (Figure 2.6(a)). An elastic material immediately will show deformation and

maintain constant strain when load is applied. The materials will come to their original shape when applied load is removed (Figure 2.6(b)). A viscous Newtonian material, at constant load, shows constant deformation until the load is removed. However, for such material, the deformation will remain the same after the load is removed (Figure 2.6(c)). Hence, viscous materials show the non-recoverable deformation, also called permanent deformation. When a creep load is applied to the viscoelastic material, it will show an immediate deformation at the beginning followed by a time dependent deformation (Figure 2.6 (d)). The immediate deformation corresponds to the elastic response of material and time-dependent deformation corresponds to viscous response of material [41].

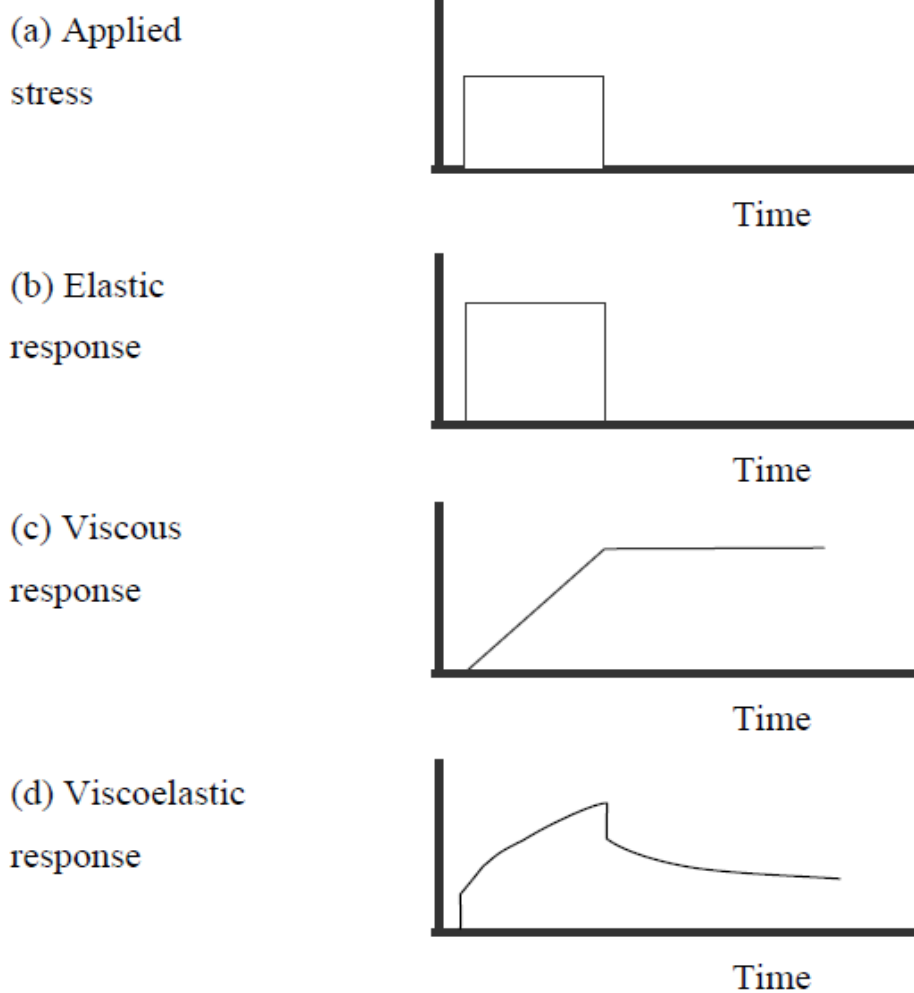


Fig 2.6: Mechanical response of elastic, viscous and viscoelastic materials under constant stress [41].

The viscous deformation component ends immediately as soon as the creep load is removed, but this deformation is not recovered. The delayed elastic deformation component is slowly recovered at a decreasing rate. Thus, a viscoelastic material shows only a partial recovery of the deformation resulting from creep loading.

If the deformation of the material is directly proportional to the applied load at any time and temperature then the material is said to be in linear viscoelastic range (LVR). The viscoelastic behavior of asphalt can be characterized by its deformation resistance and the comparative distribution of that resistance between the elastic component and the viscous component within the linear range. The relative distribution of the resistance between the elastic component and the viscous component is dependent on the asphalt cement characteristics and temperature and loading rate. For viscoelastic materials like asphalt it is difficult to model nonlinear loading responses [41].

2.5 Modification of Asphalt

Asphalt is a colloidal dispersion of asphaltenes peptized by non-polar materials which are generally referred to as resins [42]. Basically, asphalt can be classified in two types on the basis of dispersion of highly aromatic maltene fraction and asphaltenes. They are sol-type and gel-type. In sol-type asphalt, maltene and asphaltene fractions are remained in well dispersed form but in gel-type asphalt the maltene fractions are unable to disperse the asphaltenes. Schematic representations of both sol-type and gel-type asphalts are provided in Figure 2.7. Sometimes the asphaltenes agglomerate into connected structures and form a continuous network. Sol-type asphalts have better physical properties and resistance to cracking than gel-types [20-43].

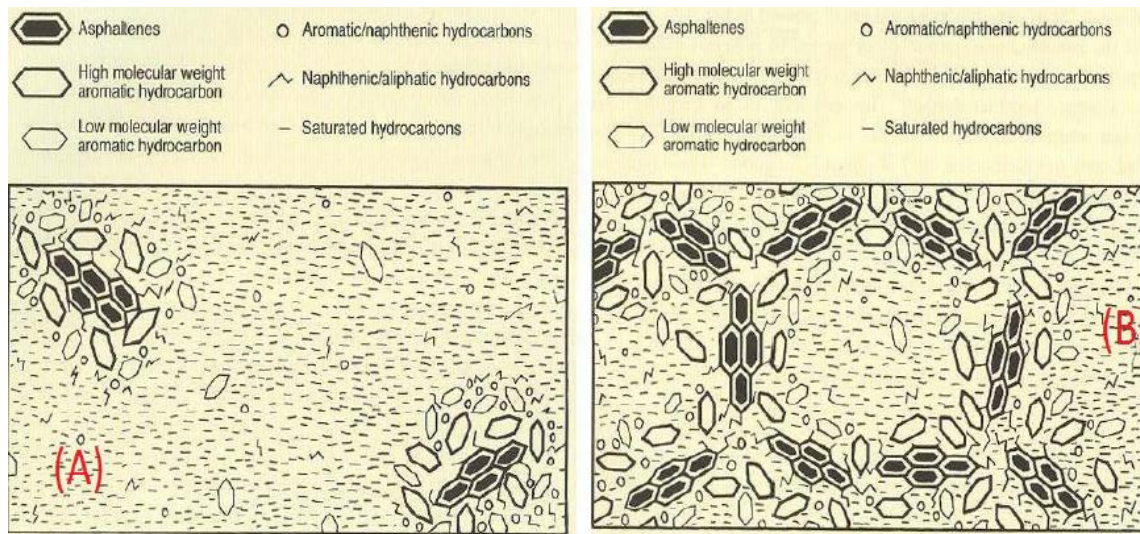


Figure 2.7: (A) Sol-type and (B) gel-type asphalts [44].

Generally, modification of asphalt is to meet the special requirements of pavements ease of road constructions, reduce the maintenance frequency, improve the useful temperature interval in service, phase stability, reduce the cost, durability by reduced hardening and also fit in the specifications like Superpave, etc. They are also expected to improve binder performance by providing good cracking resistance, moisture resistance, and good adhesion and cohesion within the pavement layers [45].

The performance of asphalt binder can be improved by selecting the suitable starting crude materials or by changing the refinery process. Many asphalt industries have introduced various types of additives to change the properties of asphalt binder so that it can give better performance on road pavements. Different types of polymeric materials are used as modifier to obtain the improved performance. Some asphalt binders could require modifiers such as polymers to meet low and high temperature requirements. Desirable characteristics of polymer modified binders

include greater elastic recovery, a higher softening point, greater viscosity, greater cohesive strength and greater ductility [46-47]. Asphalt modification process which involve natural and synthetic polymers were started as early as 1843 [48]. Some of these modifications contain polyphosphoric acids which help to increase the temperature range in which satisfactory performances can be achieved, air blowing which makes the asphalt binder hard, fluxing agents or diluents oils which soften the asphalt and other additives such as mineral acids, bases, and fillers. Even though modifiers might affect many properties, most modifiers attempt to decrease the temperature dependency and oxidation hardening of asphalt binder mixtures [3]. Various type of asphalt modifier and their examples are shown in Table 2.1.

Table 2.1: Asphalt Modifier Type [44].

S.No	Type of Modifier	Example
1	Thermoplastic elastomers	Styrene-butadiene-styrene (SBS)
		Styrene-butadiene-rubber (SBR)
		Styrene-ethylene-butadiene-styrene (SEBS)
		Ethylene-propylene-diene terpolymer (EPDM)
		Natural rubber
		Crumb tire rubber
		Polybutadiene (PBD)
		Polyisoprene
2	Thermoplastic polymers	Ethylene vinyl acetate (EVA)
		Ethylene butyl acrylate (EBA)
		Atactic polypropylene (APP)
		Polyethylene (PE)
		Polypropylene (PP)
3	Thermosetting polymers	Epoxy resin
		Polyurethane resin
4	Chemical modifiers	Organo-metallic compounds
		Sulphur
		Lignin
5	Fibres	Cellulose
		Alumino-magnesium silicate
		Glass fibre
		Asbestos
		Polyester
6	Adhesion improvers	Polypropylene
		Organic amines
		Amides
7	Anti-oxidants	Amines
		Phenols
		Organo-zinc/organo-lead compounds
8	Natural asphalts	Trinidad Lake Asphalt (TLA)
		Gilsonite
		Rock asphalt
9	Fillers	Carbon black
		Hydrated lime
		Lime
		Fly ash

2.5.1 Addition of Polymer

The addition of polymers to asphalt has been shown to improve performance. Pavements with polymer modified asphalt binders show greater resistance to rutting and thermal cracking, and decreased fatigue damage, stripping and temperature susceptibility. Polymer modified binders have been used successfully at these locations where stress is high, such as intersections of busy streets, airports, vehicle weigh stations, and race tracks [46].

Generally, two groups of polymers are used as asphalt modifiers: plastomers and elastomers. The materials which when stretched will largely remain in the stretched position after removing load are called plastomers. For example, ethylene vinyl acetate (EVA), and ethylene-acrylate (EA), polyethylene (mostly low density polyethylene, LDPE), etc. They are used in asphalt pavements to decrease permanent deformation or rutting. On the other hand, elastomers are those materials which will regain their original shape after removing the load. Elastomer materials will show the characteristics of high elongation and flexibility or elasticity, against its breaking or cracking [49]. Some example of elastomers are: styrene-butadiene rubber latex (SBR), diblock styrene-butadiene (SB) and triblock styrene-butadiene-styrene (SBS).

The addition of SBR to asphalt shows the improvement of low-temperature ductility, increases viscosity, improves elastic recovery and improves the adhesive and cohesive properties of the pavement. Water-based SBR latex is commonly used to improve bit retention in emulsions. But SBR latex has been gradually replaced by SBS because SBS is compatible with broader range of asphalts and it has greater tensile strength under strain. SBS is the mostly used polymer to modify the asphalt. SBS increases the elasticity and SBS modified asphalts are recyclable. At low

temperature SBS modified asphalt binders have found to perform better than neat binder or binder modified with chemically reactive polymer [46, 50]. Elvaloy® is another asphalt modifier that can form bonds with asphalt binder and avoid the problem of separation during storage, transport and application. It increases the pavement moisture resistance and results in modified asphalt performing better in high temperature DSR test. Good measurement of polymer contribution to the asphalt binder is the elastic recovery test [50].

2.5.2 Polyphosphoric Acid (PPA) Addition

PPA modification of paving asphalt was first reported in U.S. Patent No. 3,751,278, issued August 7, 1983 [51]. PPA is an effective and economical tool for chemical modification. It can be used alone or in combination with a polymer. With some asphalt sources, it can improve the high-temperature performance grade (PG) and could slightly improve the low-temperature PG grade. It does not oxidize asphalt. PPA provides flexibility in reaching specified dynamic shear rheometer (DSR) and elastic recovery criteria, when used with polymer. When used with acidic aggregates such as granite, PPA can enhance moisture resistance of a mix such that an antistripping reagent might not require [52]. PPA is also used to increase the softening point of a binder without lowering the penetration value. The use of such modifier produce some negative effects on long term i.e. fatigue performance according to the source of asphalt [53, 54].

The major benefits of asphalt modification include the following [55]:

- Improve binder-aggregate adhesion;
- Improve rutting resistance;
- Improve consistency;
- Improve stiffness and cohesion;

- Reduce temperature susceptibility;
- Improve flexibility, resilience and toughness; and
- Improved resistance to in-service ageing.

2.5.3 Air Blowing

The physical properties of asphalts could be modified by air blowing. It is an oxidation process which involves the blowing of air through the asphalts with short residue at a temperature of 240°C to 320°C. It is commonly employed in the production of roofing material. Blowing can improve the temperature susceptibility by giving a higher penetration for a given softening point temperature with a lower glass transition temperature [56, 57]. According to new Superpave specification, air blowing can produce very good grade asphalts, and the blowing temperature does not have serious impact on the grade span [56]. However, the long term durability is compromised by air blowing in that such binders suffer from physical and chemical hardening in service.

2.6 Test Method Specifications

2.6.1 Conventional Methods

2.6.1.1 Penetration Test

The penetration test is the oldest asphalt cement grading test. It was first developed by H.C. Bowen of the Barber Asphalt Paving Company in 1888. The basic principle of the penetration test was to determine the depth to which a truncated No. 2 sewing needle penetrates an asphalt sample under a specified condition of load, time and temperature [58].



Figure 2.8: Penetration test equipment [58].

This test method comprises the penetration of a needle into the asphalt under a standard load of 100 g, at a standard temperature of 25°C, for a standard time of 5s (Figure 2.8). This is measured in units of decimillimeters, i.e. 0.1 mm. For example, 60 Pen asphalt cement will have a penetration of the needle 6 mm at 25°C, means 60 times 0.1 mm. [59]. Lower the value of penetration harder the asphalt. The value obtained from penetration test helps to classify the asphalt on the basis of grade rather than quality. The advantage of this method is that it is cheap and gives the better result that high temperature viscosity method in terms of low temperature performance. The consistency of asphalt binder is related to temperature change by following equation.

$$\text{Log}P = AT + K \quad (1)$$

P = Penetration at temperature T.

A = Temperature susceptibility.

K = Constant.

If penetration is measured over a range of temperatures, the temperature susceptibility of the asphalt can be established. Penetration index (PI) is related with temperature susceptibility (A) by following equation.

$$\text{PI} = \frac{20(1 - 25A)}{(1 + 50A)}$$

The value of A or PI can be derived from the penetration measurements at two temperature T_1 and T_2 by following equation.

$$A = \frac{\log(\text{pen at } T_1) - \log(\text{pen at } T_2)}{T_1 - T_2}$$

The PI value can be used to determine the stiffness or modulus value at any temperature and loading time [60].

2.6.1.2 Ring and Ball Softening Point Test

This method is used to classify asphalts based on their tendency to flow at the high temperatures encountered in service. The softening point test set up is shown in Figure 2.9. According to ASTM

D36-95 method [61], asphalt is poured in two shouldered brass rings and allowed to solidify. Then steel balls of 3.5 g are placed centrally on the top of asphalt which was poured in the rings. Then it is heated at a constant rate of 5°C per minute in a liquid bath inside the beaker. Different heating media (water or glycerin or ethyl glycol) are chosen for different temperature ranges. Water is used as the preferred medium over the temperature range of 30 to 80°C, glycerin is used as the heating medium for the temperature range of 80 to 157°C, and ethylene glycol is used as the medium for the temperature range of 30 to 110°C. The average of the temperatures at which the two rings soften and allow each ball to pass through the asphalt, to fall a distance of 25 mm is noted as the softening point. The difference between the each ball temperature readings should not exceed a specified value.

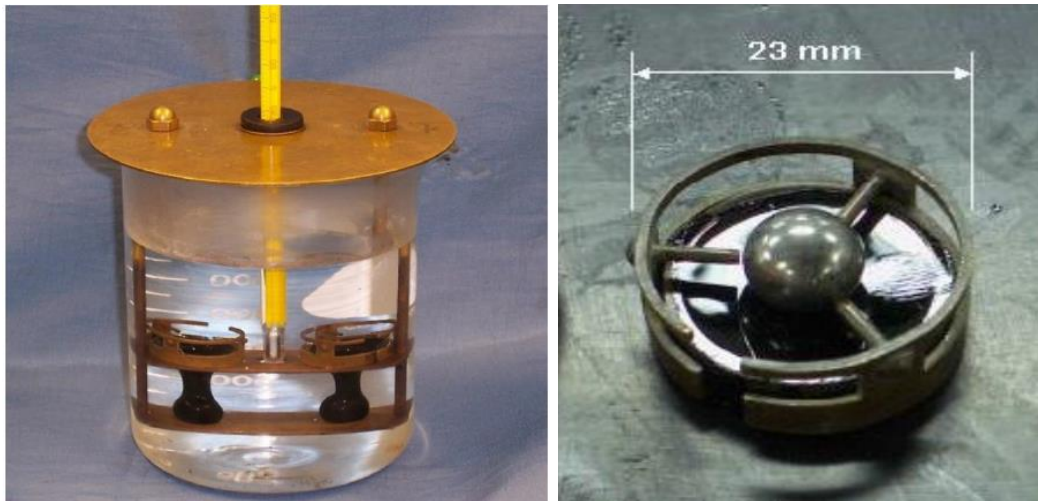


Figure 2.9: Softening point test set up [15].

2.6.1.3 Viscosity Test

Viscosity is the basic property and a measure of the resistance to flow of fluids. The viscosity test was first introduced in the early 1960s. Both the viscosity test and the penetration test are used to determine the grades of an asphalt. The advantage of the viscosity test over the penetration test is that the viscosity test measures a fundamental physical property rather than an empirical value. Viscosity is defined as the ratio between the applied shear stress and induced shear rate of a Newtonian fluid. The viscosity tests measures the time required for the asphalt cement to flow through a calibrated glass tube. Temperature-viscosity graphs are used to estimate mixing and compaction temperatures for the asphalt mix design. Viscosity tests measure the time required for the asphalt cement to flow through a calibrated glass tube [14].

2.7 Superpave Specification Tests

2.7.1 Indirect Tensile (IDT) Creep and Strength Test

The aim of the AASHTO Mechanistic-Empirical Pavement Design Guide (MEPDG) is to identify the physical cause of stresses in pavement structures and calibrate them with observed pavement performance. The two elements responsible for defining this approach to pavement design are: a mechanistic part that focuses on physical causes and an empirical part that focuses on determining the relationship by using observed performance. The MEPDG is mainly based on the empirical observations from AASHTO (American Association of State Highway and Transportation Officials) road test that began in the 1950s and it is designed to update the 1993 AASHTO Guide for Design of Pavement Structure. In mechanistic-empirical design, the design of the pavement structure is supposed initially on trial basis, along with inputs for traffic and climate. In combination with the MEPDG research project, software was also developed to support in

organizing and performing these design calculations. MEPDG software can compute according to the response of trial design to the load and environmental stresses produced by these inputs. This enables to an estimate the degree of damage the pavement will tolerate over time, in terms of pavement distresses and worsening in ride quality [62].

The AASHTO MEDPG software treats a pavement as a multi-layered elastic system with the following assumptions [63-64]:

- Homogeneous material properties within each layer;
- Each layer has a finite thickness, except the lower layer;
- All layers are infinite in the lateral directions;
- Each layer is isotropic;
- Full friction is developed between each layer;
- Surface shearing forces can be neglected; and
- Stress solutions are characterized only by the elastic modulus and Poisson's ratio.

Two weeks or one month increments are used for calculations. Within each increment, all parameters like moduli, traffic conditions, and weather factors are held constant. For good results accurate traffic data and at least 1 year's weather data is required. Critical stress and strain values are output for the end of each increment, and are added over all increments. A detailed description of the computation process is as follows [64-65]:

- Creep compliance at -20, -10, and 0°C and tensile strength at -10°C are entered into the software, since the model is based on linear visco-elasticity;

- Creep compliance master curves are developed and fit to a Prony series as well as a power law model to determine key fracture parameters for use in the model;
- Thermal stress is predicted at any given time and depth by converting the creep compliance to relaxation modulus values and combining with climate data;
- Crack growth is estimated using Paris' law, which uses the fracture parameters derived earlier. This law allows for computation of the stress intensity and fracture properties of the asphalt; and
- Physical cracking is obtained from stress intensity. This is done with calibrated models developed using long-term pavement performance data for a wide range of pavement designs, traffic loads, and climates. The default acceptance criteria is 1000 feet of thermal cracking per mile (190 m per km). It should be noted that calibration of this model was done on 500 feet sections, and extrapolated to a mile.

This approach assumes a maximum amount of cracking of 800 m per km of pavement. However, the model cannot predict more than approximately half of this value since at this point, the crack depth is predicted to equal the layer thickness. The standard error of the results can be estimated using the empirical relation shown in Equation 1. The standard error and predicted thermal cracking are in feet per 500 feet of pavement [63-64].

$$\text{Standard Error} = 0.2474 * \text{predicted thermal cracking} + 10.61 \quad [1]$$

Creep compliance is defined in T 322-07 as “the time-dependent strain divided by the applied stress”. Creep compliance testing is non-destructive in that the load is controlled so that upper linear elastic boundary of the Hot Mix Asphalt (typically 500 microstrain) is not exceeded,

therefore each specimen can be tested at several temperatures. However, the load must be large enough to produce sufficient horizontal deformations (≥ 0.00125 mm or 33 microstrain based on a 38 mm gauge length) such that noise in the data acquisition process is insignificant [65]. Tensile creep and tensile strength test data are required for Superpave mixture to determine the master relaxation modulus and fracture parameters. This information is used to calculate the thermal cracking of Hot Mix Asphalt. The master relaxation modulus curve controls thermal crack development while the fracture parameter defines the mixture's resistance to fracture. The values of different parameters like creep compliance, tensile strength and Poisson's ratio can be used to calculate the low temperature thermal cracking potential of concrete asphalt. Tensile creep data may be used to evaluate the relative quality of materials [66].

Creep compliance is calculated as a function of the horizontal and vertical deformations, the gauge length over which these deformations are measured, the dimensions of the test specimen, and the magnitude of the static load. Creep compliance determination, as defined in T 322-07, is given as follows [67]:

$$D(t) = \frac{\Delta X_{tm, t} \times D_{avg} \times b_{avg}}{P_{avg} \times GL} \times C_{cpl} \quad (1)$$

Where:

$D(t)$ = creep compliance at time t (kPa^{-1});

GL = gauge length in meters (0.038 m for 150 mm diameter specimens);

D_{avg} = average diameter of all specimens [typically 3] (nearest 0.001 m);

b_{avg} = average thickness of all specimens [typically 3] (nearest 0.001 m);

P_{avg} = average creep load (kN)

$\Delta X_{tm, t}$ = trimmed mean of the normalized, horizontal deformations (nearest 0.001 m) of all specimen faces [typically 6] at time t ; and

$$C_{\text{cmpl}} = \text{correction factor} = 0.6354 \times \left(\frac{X}{Y}\right)^{-1} - 0.332 \quad (2)$$

$\frac{X}{Y}$ = absolute value of the ratio of the normalized, trimmed mean of the horizontal deformations (i.e. $\Delta X_{tm,t}$) to the normalized, trimmed mean of the vertical deformations (i.e. $\Delta Y_{tm,t}$) at a time corresponding to $\frac{1}{2}$ the total creep test time [typically 50 s] for all specimen faces.

Tensile strength can be calculated by equation (3):

$$S_{t,n} = \frac{2P_{f,n}}{\pi * b_n * D_n} \quad [3]$$

Where $S_{t,n}$ is the tensile strength, $P_{f,n}$ is the load at failure, b_n is the thickness, and D_n is the diameter of sample n.

2.7.2 Dynamic Shear Rheometer Test

Asphalt binders are viscoelastic. The behaviour depends on the both loading time and temperature. To evaluate both time and temperature a suitable test is the DSR test. DSR is used to quantify both elastic and viscous properties. DSR measures the rheological properties (complex shear modulus and phase angle) at intermediate to high temperatures, when used for asphalt binders. This makes it a suitable method for characterizing asphalt binders in the in-service pavement temperature range.

DSR is used to characterize both viscous and elastic behaviour by measuring complex shear modulus (G^*) and phase angle (δ) of asphalt binders. G^* can be considered as the binder's total resistance to deformation when repeatedly sheared. It consists of two components: elastic (recoverable) and viscous (non-recoverable). Phase angle (δ) is the interval between applied shear stress and resulting shear strain. It also indicates the relative amount of elastic and viscous

component. The larger the phase angle the more viscous the materials. The limiting value of phase angle (δ) are 0 degree for purely elastic and 90 degree for purely viscous [67].

Usually, in a DSR test a sample of asphalt binder is placed between two parallel steel plates. The top plate is oscillated by a precision motor with a controlled angular velocity, w , while the bottom plate remains fixed. DSR is used to calculate shear stress and shear strain by measuring torque and angle of rotation [68].

The oscillatory strain, γ ,

$$\gamma = \gamma_o \sin wt \quad (1)$$

Where, γ_o is the peak shear strain and w is the angular velocity in radian/second

The shear stress, τ ,

$$\tau = \tau_o \sin (wt + \delta) \quad (2)$$

Where, τ_o is the peak shear stress and δ is the phase shift angle.

Then, Complex Shear Modulus can be determined as $G^* = \tau_o / \gamma_o$ (3).

Complex shear modulus, G^* determines the resistance of material to the deformation under applied shear stress. The phase angle, δ , is related to the time lag between the applied stress and the resulting strain, and it can be expressed as the ratio of viscous or loss modulus, G'' , to the storage or elastic modulus, G' .



Figure 2.10: Dynamic Shear Rheometer.

For high temperature grading, 25 mm diameter plate geometry and a 1 mm gap is maintained to run the test. Sample is poured in a silicon mold and solidified before loading to the bottom plate. A trimming tool is used to trim excess sample. Then testing parameters like frequency, which is speed of oscillation (one cycle), generally 10 radians/second, loading time, and test temperature, etc., are given to the software to run the testing. Strain values should be small and remain in the linear viscoelastic range. The rheometer produces the results automatically by using the software. According to AASHTO specification, the high temperature PG grades decided on the following values, $G^*/\sin\delta > 1.00$ kPa for fresh and $G^*/\sin\delta > 2.20$ kPa for RTFO aged samples. An 8 mm diameter plate geometry and 2 mm gap is maintained to run the intermediate grading (fatigue grading) test. As per the AASHTO specification, the intermediate temperature PG grades decided on $G^*\sin\delta$ less than 5000 kPa for PAV residue. Finally, DSR measurements at high temperatures are related to rutting and at intermediate temperatures are related to thermal cracking [40].

2.7.3 Bending Beam Rheometer Test

The Bending Beam Rheometer (BBR) test provides a measure of low temperature stiffness and relaxation properties of asphalt binders. These parameters reflect an asphalt binder's ability to resist low temperature cracking. The heated asphalt binder is poured in to molds and allowed to solidify. Trimming has to be done before conditioning in an ethanol bath. After 1 hour of thermal conditioning, the asphalt beam is placed on supports to apply a three point load. After the application of a preload of 35 mN, a seating load of 980 mN is applied for 1 second, and allowed for a 20 second recovery period. The graph of load and deflection versus time is plotted continuously. The rheometer software produces the results automatically. The creep stiffness (S), which is the binder resistance to creep loading, and creep rate (m), which is the asphalt stiffness change with time during the application of load, are measured by using the BBR instrument. The deflection of the beam is recorded when load is applied during this period, and creep stiffness of the asphalt can then be calculated by the following equation [40]:

$$S(t) = PL^3 / 4bh^3\delta(t) \quad (4)$$

Where: S (t) = creep stiffness at time, t

P = applied load, 100 g

L = distance between beam supports, 102 mm

b = beam width, 12.5 mm

h = beam height, 6.25 mm,

$\delta(t)$ = deflection at time, t

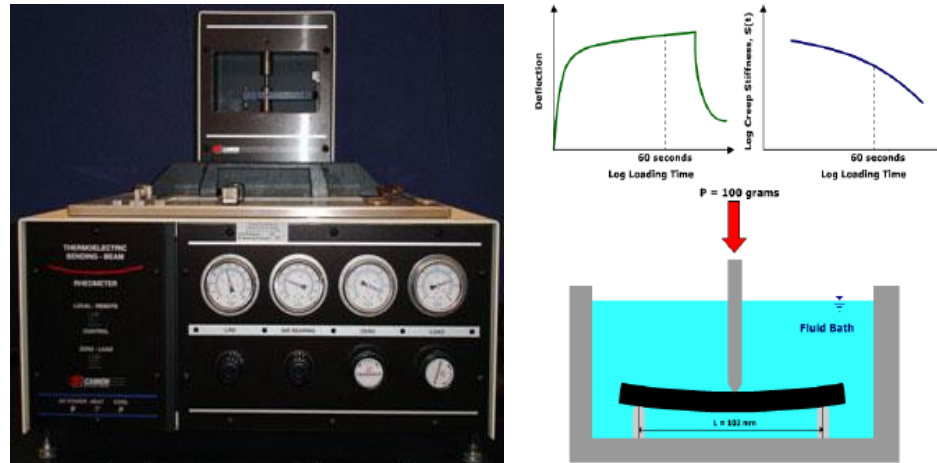


Figure 2.11: Bending Beam Rheometer [15].

According to the Superpave binder specification, the bending beam rheometer test is to be conducted at 10°C above the expected minimum pavement temperature, T_{\min} , the stiffness at which is approximately equal to its stiffness at T_{\min} after 2 hours loading time, which is related to low temperature cracking potential. The Superpave binder specification requires the stiffness at the test temperature after 60 seconds to be less than 300 MPa, to control low-temperature cracking. The slope of the log stiffness versus log time curve gives the m-value at a specified time. As per the AASHTO specification, the low temperature PG grades are decided based on the limiting temperature where stiffness < 300 MPa or m-value > 0.300 for the PAV residue [40]. A higher m-value indicates that asphalt creep at a faster rate to reduce the thermal stress and in turn desirable to reduce low-temperature cracking [68]. Existing method contains some drawbacks like lack of sufficient ageing time and high strain testing. Hence, a new improved method was developed over the last 10 years at Queen's University.

2.8 Improved Ministry of Transportation Ontario (MTO) Test Methods

The Superpave specification follows insufficient aging and conditioning time and low strain testing methods to predict asphalt performance. Following new sets of testing methods has been developed by the collaboration work of the Ontario Ministry of Transportation with Queen's University.

1. Extended Bending Beam Rheometer (eBBR) test (LS-308);
2. Double Edge Notched Tension (DENT) test (LS-299);

2.8.1 Extended Bending Beam Rheometer (eBBR) Method LS-308

Physical hardening of asphalt cement is different at different temperatures at low temperature and can increase over time. In the regular BBR test the conditioning time is one hour but in extended BBR test the conditioning time is one day and three days. The poor quality asphalts which contain large quantities of wax and unstable asphaltene dispersion shows severe grade loss in extended BBR test. In the extended BBR the conditioning temperatures T₁ and T₂ are fixed as follows:

$$T_1 = T_{\text{design}} + 10 \text{ and}$$

$$T_2 = T_{\text{design}} + 20.$$

LS-308 conditions at 10°C and 20°C above the actual grade temperature (i.e. pavement design temperature) for periods of 1 h, 24 h, and 72 h to simulate the effect of extended exposure to two different cold temperatures [69]. Exact grade of pass and fail temperatures are determined according to AASHTO M320 criteria by interpolation which involves plotting the grade on a semi-logarithmic scale [70]. This method helps to get a high degree of confidence to prevent thermal cracking.

2.8.2 Double-Edge Notched Tension (DENT) Test LS-299

The test is conducted after thermal conditioning to determine the essential work of failure, the plastic work of failure, and an approximate critical crack tip opening displacement (CTOD), at a specified temperature and rate of loading. Samples are prepared in double-edge-notched shape with ligaments, i.e. distances between two opposing notches of 5 mm, 10 mm, and 15 mm in length, by pouring in molds and allowed to solidify. Samples are trimmed then conditioning was done at room temperature and in a water bath for 3 hours at the test temperature like 15°C before testing. Then samples are pulled until they fail in a water bath [71].

The DENT test is based on the Essential Work of Fracture (EWF) method. The assumption is made that the total work of failure (W_t) is the sum of an essential work of failure (W_e) and a non-essential work of failure (W_p).

W_t can be determined from the total area under the force-displacement curve:

$$W_t = W_e + W_p \quad (5)$$

Essential work of failure (W_e) and non-essential work of failure (W_p) can be determined by the following equations:

$$W_e = w_e \times LB \quad (6)$$

$$W_p = w_p \times \beta L^2B \quad (7)$$

Where,

w_e = specific essential work of fracture (J/m^2),

w_p = specific plastic work of fracture (J/m^2),

L = the ligament length in the DENT specimen (m),

B = the thickness of the sample (m), and

β = the shape factor of the plastic zone, which is geometry dependent.

If we substitute equations 6 and 7 in 5,

$$W_t = (w_e \times LB) + (w_p \times \beta L^2 B) \quad (8)$$

By dividing equation (8) by the cross-sectional area of the plastic zone (LB),

$$W_t/LB = w_t = w_e + w_p\beta LB \quad (9)$$

Where, w_t = specific total work of fracture (J/ m^2).

Specific total work of failure, w_t , versus the ligament length, L , in equation (9), gives a straight line with slope and intercept on the w_t axis. The w_e helps to predict fatigue cracking resistance and to determine the CTOD.

$$\delta_t = w_e / \sigma_n \quad (10)$$

Where, δ_t = the crack tip opening displacement parameter (m), and

σ_n = the net section stress or yield stress (N/m^2), determined from the 5 mm ligament length of the DENT mould.

High correlations exist between the CTOD and the fatigue properties of the asphalt cement. CTOD can be used to rank the performance and determine a high correlation with cracking distress.

Chapter 3

MATERIALS AND EXPERIMENTAL

3.1 Materials

The materials used in this study were obtained from Ministry of Transportation Ontario (MTO) and City of Kingston contracts. Two contracts were obtained from City of Kingston and six contracts from MTO. More information about the sample contracts is provided in Table 3.1.

Table 3.1: Sample contracts.

Highway	Region	PG Grade
JCB (4 and 6% air voids)	Kingston	64-28 XD
Burbrook Road	Kingston	58-28 XD
401-1	Central	70-28
28	Eastern	58-34 P
401-2	Eastern 1	64-28 D
401-3	Eastern 2	64-34
417	Eastern	64-34
406	Central	64-28 D

3.2 Experimental

3.2.1 Sample Preparation for IDT

3.2.1.1 Ageing

Hot mix asphalt concrete briquettes were prepared in the laboratory according to standard procedures using a Pine Instruments gyratory compactor. Boxes of each contract mix were placed in a preheated oven at 120°C about 20 hours before mixing. Ageing time and temperature for different contracts is shown in Table 3.2.

Table 3.2: Ageing of different sample contracts.

Highway No.	Region	Aging Time (Hours)	Aging Temperature (°C)	Compaction Temperature (°C)
JCB	Kingston	20	120	145
JCB	Kingston	19	120	145
Burbrook Road	Kingston	21.5	120	145
401-1	Central	20.5	120	145
401-2	Eastern-1	20.5	120	145
401-3	Eastern-2	20.5	120	145
28	Eastern	20	120	145
417	Eastern	21.5	120	145
401-2	Eastern-1	6	145	145
401-3	Eastern-2	6	145	145
406	Central	21.5	120	145

3.2.1.2 Mixing

A bucket mixer, preheated in an oven of equal temperature with the mixture, was used for mixing as shown in Figure 3.1. Heated soft asphalt mix was poured in to the bucket mixer and mixed thoroughly. A paper disk was placed on the bottom plate of each gyratory mold, the mold was placed on a scale and tared to zero. The required weight of hot mix asphalt was placed into the molds. The molds were tamed using a rubber mallet and a rod for proper compaction. Another paper disk was placed on top of the hot mix, and then the mold was put in the oven at 145°C for 2 hours for normal heating. For minimal heating, sample mixes were put in the preheated oven at 145°C for 3 hours before mixing.



Figure 3.1: Bucket mixer.

3.2.1.3 Compaction

All cores, which contain calculated amount of material, were compacted using the Pine Instruments AFG 2 Superpave™ Gyrotory Compactor as shown in Figure 3.2. The compaction was done according to AASHTO T 312 [72], where compaction pressure, compaction angle and speed of gyration were set to the required values.



Figure 3.2: Pine Instruments AFG 2 Superpave™ gyrotory compactor.

The molds were removed from the oven and allowed to cool to 130°C before compaction. After compaction, the molds were allowed to cool to 80°C, so the sample could be extruded with the aid of the gyrotory ram. The specimen was labelled and allowed to cool to room temperature in preparation for cutting.

3.2.1.4 Cutting and Air Voids Determination

Each briquette were cut in to two or three disks (samples) of 50 or 38 mm using the saw blade as shown in Figure 3.3.



Figure 3.3: Struers Automated Cutting Saw.

Immediately after cutting, the different weights (weight in water and weight of saturated surface dry) of sample were determined. The samples were left for perfect drying after which the dry weight was determined. Bulk specific gravities (G_{mb}) and actual air voids of each cut samples were then determined [73], as follows:

$$\% \text{ Air Voids} = (G_{mm} - G_{mb} / G_{mm}) \times 100 \quad (11)$$

Where, G_{mm} = maximum specific gravity; and

G_{mb} = bulk specific gravity.

Bulk specific gravity is given by:

$$G_{mb} = (\text{dry weight} / \text{weight of saturated surface dry-weight in water}).$$

3.2.2 Indirect Tensile Creep

Each IDT specimen was measured (three thickness and two diameter measurements taken and then averaged). Four magnetic stubs were glued onto each face of the disks for attachment to the strain

gauges. The specimens were conditioned for two hours at the test temperature. Extensometers were attached to each magnetic stub on both sides of the specimens. The procedure detailed in AASHTO standard test T322-07 [74] was followed to obtain the deflection in both vertical and horizontal directions for each sample. Constant loads of 8000, 6000, 4000, and 2000 N were applied using an MTS load frame (shown in Figure 3.4) to obtain the creep compliances at -30, -20, -10, and 0°C, respectively. At least three discs were tested at each temperature. The test was also repeated for some discs after 72 hours of physical hardening/aging at -10°C.

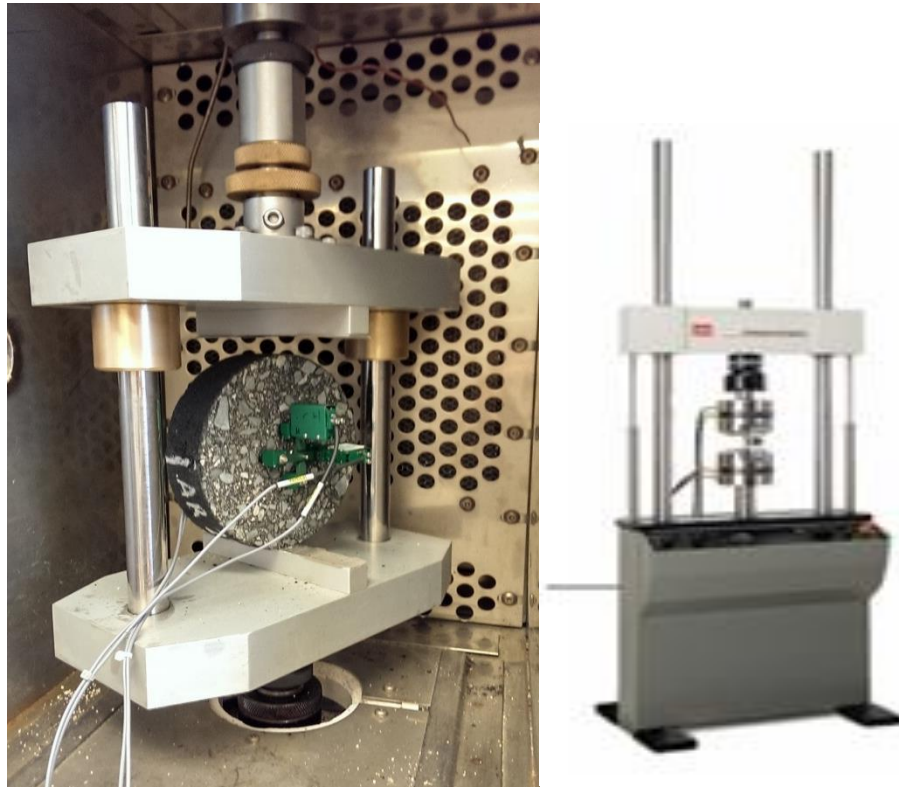


Figure 3.4: Sample loading fixture and test frame.

A trimmed mean approach was used, where the highest and lowest deflections in both the vertical and horizontal directions were discarded. This helped to decrease the coefficient of variation for the measurements. The trimmed mean of the vertical and horizontal displacements was calculated using equations 12 and 13:

$$\Delta X_t = \frac{\sum_{j=2}^{N-1} \Delta X_j}{N-2} \quad (12)$$

$$\Delta Y_t = \frac{\sum_{j=2}^{N-1} \Delta Y_j}{N-2} \quad (13)$$

Where ΔX_t and ΔY_t are the horizontal and vertical trimmed mean displacements (mm), respectively, ΔX_j and ΔY_j are the displacement values sorted in increasing order, and N is the total number of samples.

Poisson's ratio was calculated according to Equation 14:

$$\nu = -0.10 + 1.480 \left(\frac{\Delta X_t}{\Delta Y_t} \right)^2 - 0.778 \left(\frac{b_{avg}}{D_{avg}} \right)^2 \left(\frac{\Delta X_t}{\Delta Y_t} \right)^2 \quad (14)$$

Where ν is Poisson's ratio, b_{avg} is the average sample thickness (m), D_{avg} is the average sample diameter (m), and

$$0.05 \leq \nu \leq 0.50$$

The creep compliance correction factor was computed using equation 15:

$$C_{cmpl} = 0.6354 \left(\frac{\Delta Y_t}{\Delta X_t} \right) - 0.332 \quad (15)$$

Where C_{cempl} is the creep compliance correction factor.

The creep compliance was calculated using equation 16:

$$D(t) = \frac{\Delta X_t * D_{avg} * b_{avg}}{P_{avg} * GL} * C_{cempl} \quad (16)$$

Where $D(t)$ is the creep compliance as a function of time (kPa^{-1}), P_{avg} is the average force (N), and GL is the gauge length (0.038 m for a 150 mm diameter specimen).

3.2.3 Indirect Tensile (IDT) Strength

Specimens were loaded to failure at a rate of 12.5 mm/min as specified in AASHTO test method T322-07 [74]. Failure data was obtained from two specimens at -20 and -10°C, for a total of four failure samples, after three hours of aging at the test temperature. The test was repeated on select asphalt mixes after 72 hours of aging at -10°C. The tensile strength was determined according to equation 17:

$$S_{t,n} = \frac{2P_{f,n}}{\pi * b_n * D_n} \quad (17)$$

Where $S_{t,n}$ is the tensile strength, $P_{f,n}$ is the load at failure, b_n is the thickness, and D_n is the diameter of sample n.

3.3 Extraction of Binder

Failed disks were submerged in an excess of toluene and left for enough time to separate the asphalt binder from the aggregate. After removal of the aggregate, the asphalt was recovered by rotary evaporation. Recovered binder was used for different tests like BBR, DSR, DENT, XRF and FTIR.

3.4 Regular Bending Beam Rheometer Test [AASHTO M320]

The BBR measures the binder stiffness by the deflection or creep at constant load and temperature, that stiffness was used to predict the low temperature cracking. Recovered asphalt binders were heated, then stirred with glass rod to make sure the sample is homogenous and to remove any air bubble present before pouring into the molds. Bubble free binder was poured into the molds and cooled about 45 to 60 minutes. Trimming was done before conditioning in an ethanol bath. Beams were conditioned at each test temperature for 1 hour in an alcohol bath prior to testing. At least two replicates were tested by recording the deflection as a function of time as a response to a constant applied load using a Cannon BBR. Test temperatures were -30, -20, -10, and 0°C, with the load varying to ensure sufficient deflection without damage. The graph of load and deflection versus time was plotted continuously up to 240 seconds. The deflection of asphalt beam in typical BBR is as shown in Figure 3.5 (a). The rheometer software produced the results automatically. The creep stiffness (S), which is the binder resistance to creep loading, and creep rate (m), which is the asphalt stiffness change with time during the application of load, were measured by using the BBR instruments. The creep stiffness should be a minimum of 300 MPa at 60 second loading and m-value should maximum 0.3 at 60 second loading time to prevent from low temperature cracking according to the AASHTO M320 specification. The measurements of creep stiffness and m-value are shown in Figures 3.5(b) and (c) respectively.

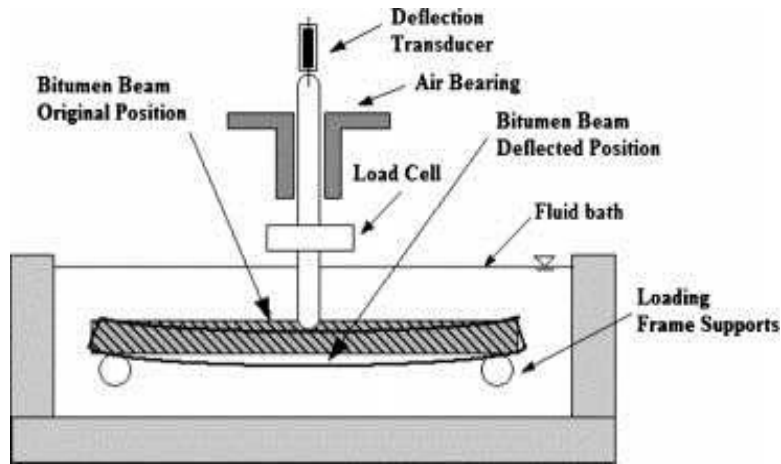


Figure 3.5(a): Deflected Asphalt Beam on Bending Beam Test [75]

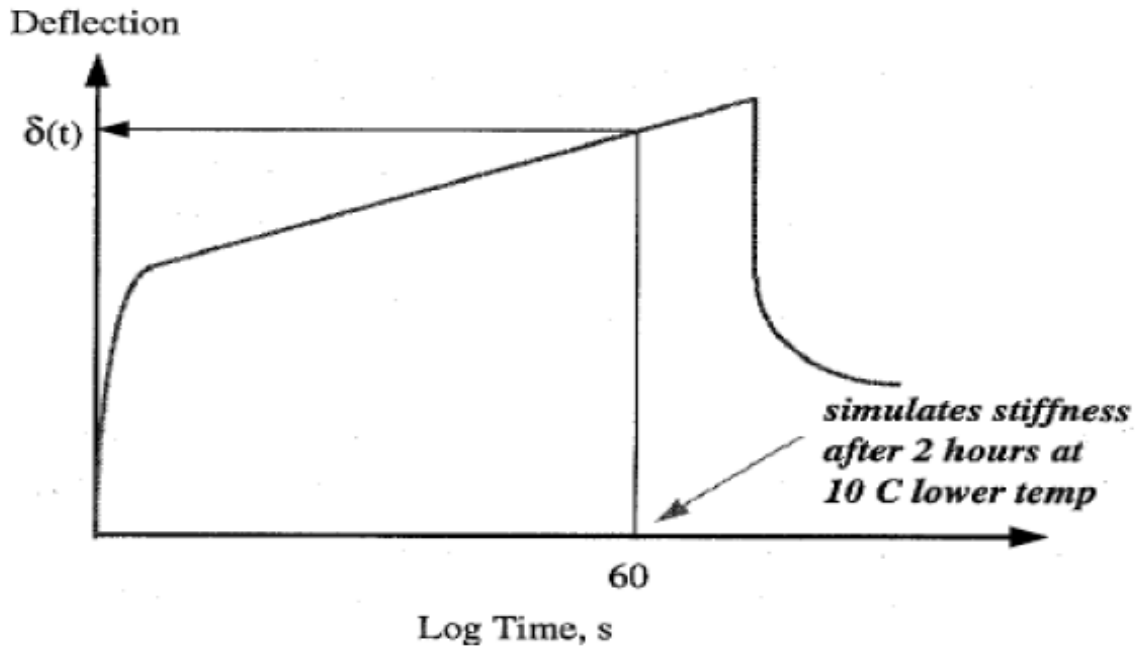


Figure 3.5(b): Creep stiffness of asphalt binders based on change in deflection with time.

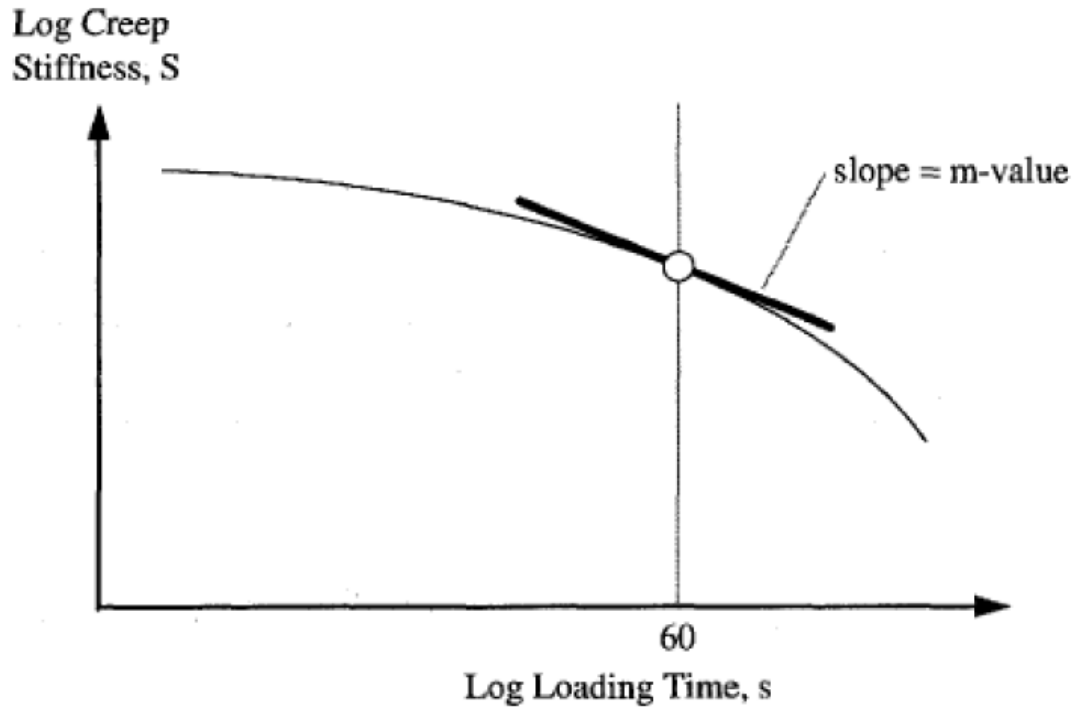


Figure 3.5 (c): Evaluation of m-value of asphalt binders.

3.5 Extended BBR Testing (MTO LS-308)

After finishing regular BBR test, all the binder beams were conditioned at -10°C for 72 hours and tested at -30 , -20 , -10 and 0°C . Exact grade of pass and fail temperatures are determined according to AASHTO M320 criteria by interpolation which involves plotting the grade on a semi-logarithmic scale [70].

3.6 Dynamic Shear Rheometer (DSR) Test

DSR determines the rheological properties like complex shear modulus, G^* (elastic component), and phase angle, δ (viscous component), of fresh, RTFO, and PAV-aged asphalt samples, for intermediate and high temperature performance grading [76]. DSR is used to measure the torque and angle of rotation to calculate the shear stress and shear strain. [68].

Recovered asphalt binder was used to find the high temperature and intermediate temperature grade. High temperature grade is supposed to control rutting. A 25 mm diameter plate geometry and a 1 mm gap was maintained to run the test. Sample was heated in oven then poured in a silicon mold and solidified before loading to the bottom plate. Trimming tool was used to trim the excess sample. Then testing parameters like frequency, which is speed of oscillation (one cycle), ranging from 0.1 to 10 radians/second, loading time, and test temperature, etc., were given to the software to run the testing. An 8 mm diameter plate geometry and 2 mm gap was maintained to run the intermediate temperature grade testing for the control of fatigue cracking. As per the AASHTO M320 specification, the high temperature PG grades are decided based on the $G^*/\sin \delta > 2.20$ kPa for high temperature testing and the intermediate temperature PG grades decided on $G^*\sin \delta$ less than 5,000 kPa.



Figure 3.6: DSR sample (A) and Spindles (B) [15]

3.7 Double Edge Notch Tension (DENT) test

Double-edge-notched tension (DENT) test is used to determine the ductile fracture or failure and fatigue cracking of asphalt binder at low temperature. The brass molds are assembled on base plates. Thin film sheet and coating of thin layer of a mixture of talc powder with glycerol or grease is used on the molds and plates to prevent the test material from sticking on the mold. Asphalt binder was heated in oven. Sample was stirred and rapidly poured in to six molds having ligament lengths 5mm, 10mm and 15mm. Molds were cooled to solidify binder then samples were trimmed with hot spatula. Conditioning was done on water bath at temperature 15°C for 3 hours. The sample is removed from the plate by a shearing action between specimen and plate, avoiding any bending of the test specimen. Then side pieces of mold are removed carefully without distortion or fracture the specimen. The rings at each end of the clips are attached to the pins or hooks in the testing machine. Then samples are pulled in a water bath at isothermal condition until they failed. The essential work of fracture and the plastic work of fracture were determined at a constant temperature of 15°C and loading rate of 50 mm/min. CTOD can be used to rank the performance and determine a high correlation with cracking distress.

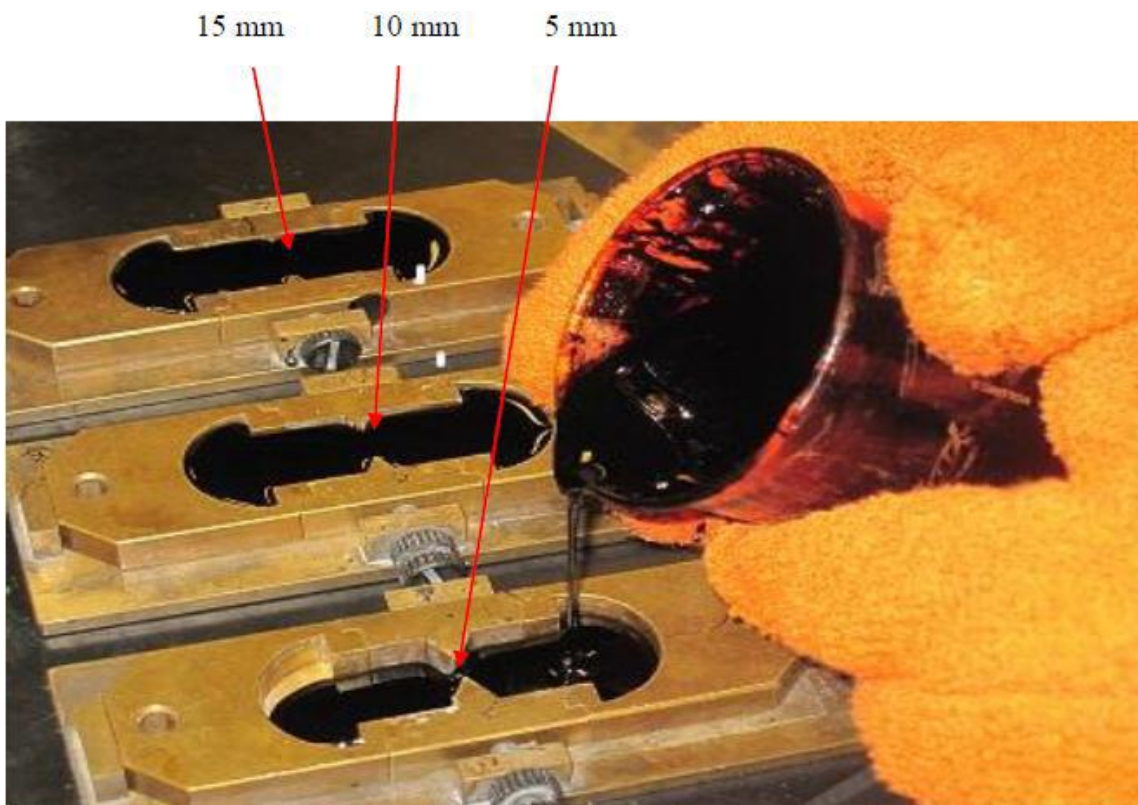


Figure 3.7: DENT sample preparation [27].

3.8 Fourier Transform Infrared Spectroscopy (FTIR)

KBr disks were heated on a hot plate set to 140°C. A very small amount of recovered asphalt was spread on the heated disk to form a uniform and thin coating. This disk was scanned using a Perkin Elmer 400 series FTIR from 4,000 to 450 cm^{-1} . The asphalt coating was applied thin enough to ensure the characteristic CH peak between 3121 cm^{-1} and 2746 cm^{-1} did not exceed an absorbance of 1.2 A.U. This was repeated for all recovered asphalt samples [63].

3.9 X-Ray Fluorescence (XRF)

A piece of recovered asphalt approximately one cm² by a few mm thick was placed in a Ziploc bag for analysis. The sample was placed on an X-ray fluorescence analyser and scanned. This was repeated for all samples, along with a waste engine oil sample obtained from a western Canadian supplier for reference [63].

Chapter 4

RESULTS AND DISCUSSIONS

4.1 IDT Creep and Strength Testing

The creep compliance curves are obtained by plotting the creep compliance for all temperatures as a function of the logarithm of time. Figure 4.1 represent the typical creep compliance curve. At lower temperatures, creep compliance is low since asphalt behaves almost brittle and creep compliance increases with temperature.

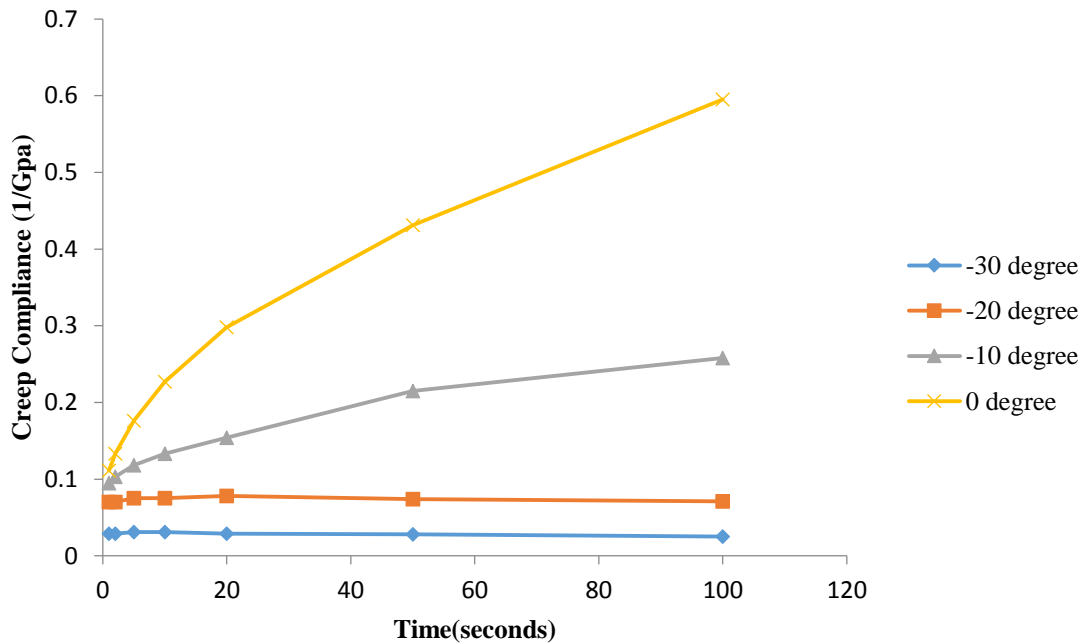


Figure 4.1: Creep Compliance curve at different temperatures.

Creep compliance data for all contracts are shown in Figure 4.2 in the form of creep compliance master curves. The temperature curves are shifted to obtain a single continuous curve. The curve

at -20°C remains unshifted as the reference, while data at temperatures above -20°C are shifted to the right, and temperatures below -20°C (if applicable) are shifted to the left.

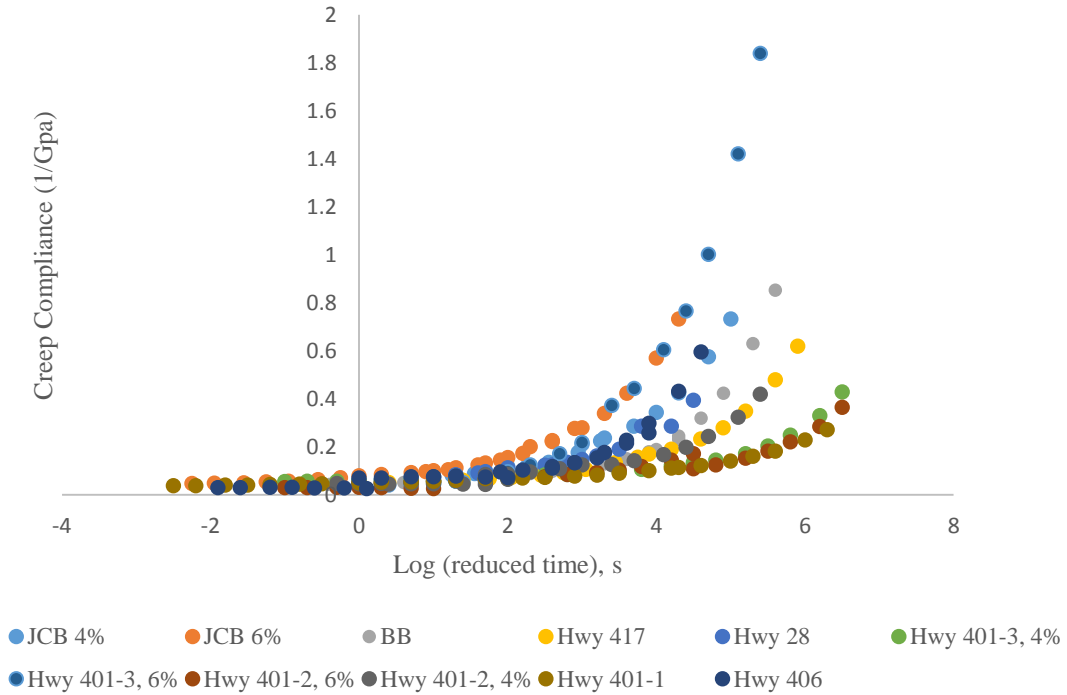


Figure 4.2: Creep compliance master curves for tested samples.

Smooth creep compliance master curves show better quality asphalt mix. Among Highway 401 series, 401-3 is found to be most compliant while 401-2 and 401-3 are the stiffest of those tested. High creep compliance is desirable as this provides the asphalt mixture to better relax, relieving accumulated stress during cold periods [77].

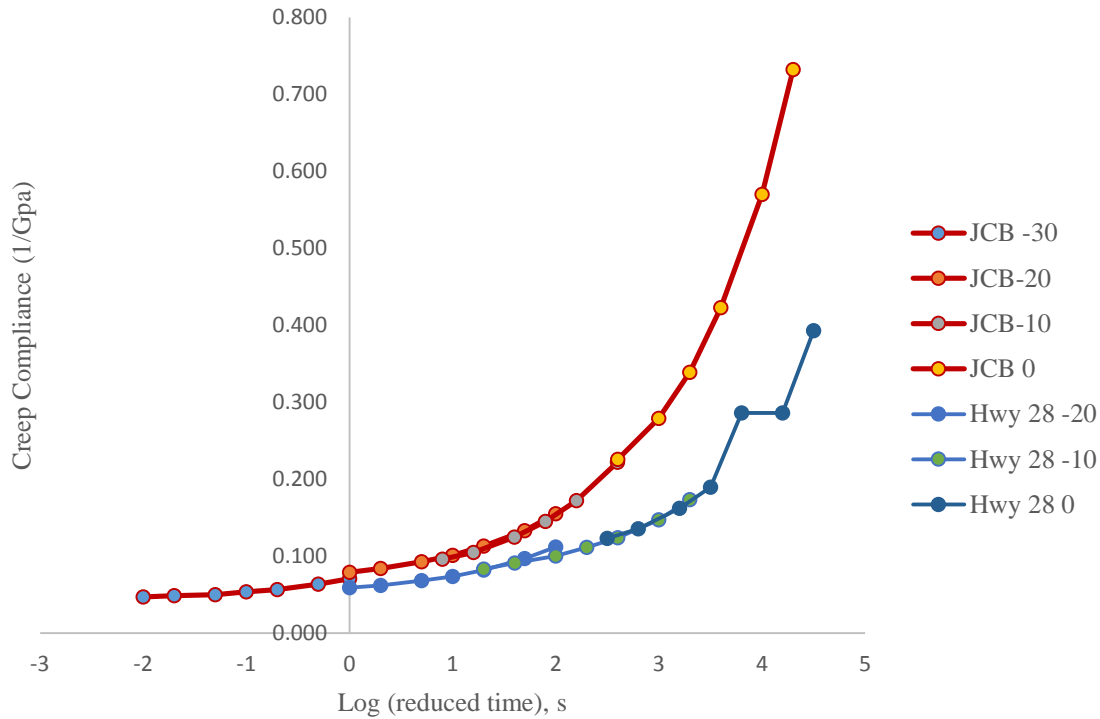


Figure 4.3: Creep compliance master curves Hwy 28 and JCB.

From Figure 4.3 it is found that smoothness of creep compliance master curve for JCB sample is better than Hwy 28 sample. So quality of JCB sample mix is better than quality of Hwy 28 sample mix.

IDT creep compliance values were also obtained for JCB samples at 4 and 6% air voids, as well as for Hwy 28 samples after three days of physical hardening/aging at -10°C . Comparisons of the master curves for these samples after three hours and three days of aging are presented in Figures 4.4, 4.5 and 4.6. JCB at 4% air voids and Hwy 28 samples stiffened with additional low temperature aging, as was expected. However, JCB samples at 6% air voids became more compliant after additional low temperature aging. This may be due to the difference in coefficients

of thermal expansion for the aggregate and the asphalt binder. The extra aging might have caused micro voids to grow, damaging the samples [78]. This damage could have led to the apparent softening of the sample.

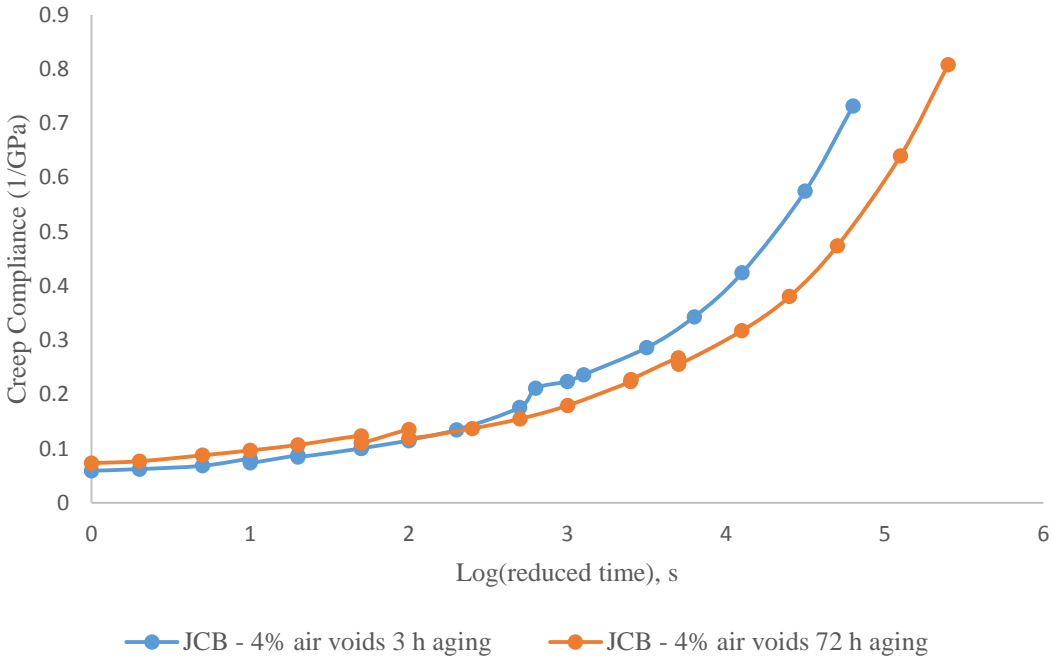


Figure 4.4: Comparison of creep compliance master curve after 3 and 72 h ageing for JCB -4% air voids.

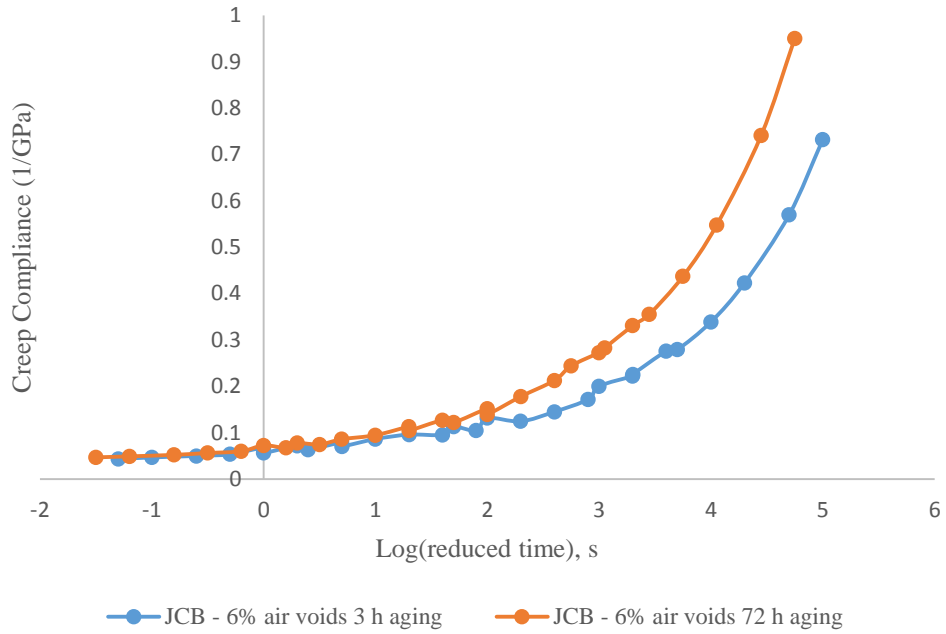


Figure 4.5: Comparison of creep compliance master curve after 3 and 72 h ageing for JCB -6% air voids.

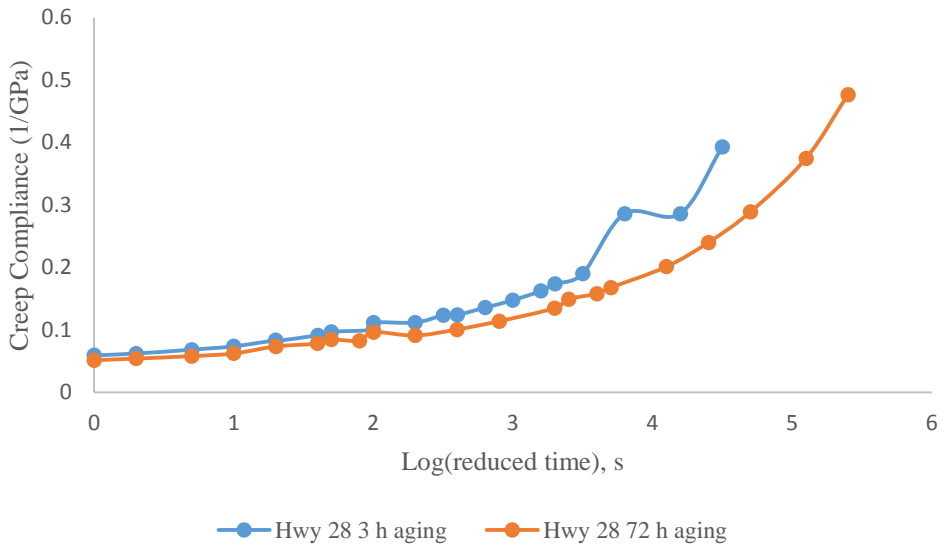


Figure 4.6: Comparison of creep compliance master curve after 3 and 72 h ageing for Hwy 28.

The coefficients of variation (CoV) for the creep compliances is found to be ranging from 12-21% which is higher than the 8-11% reported by other laboratories using similar methods [79]. Since the test method used was the same, the increased inconsistency for these results could be due to some error on sample preparation and test equipment.

Tensile strengths results are summarized in Figure 4.7. High tensile strength is preferred for performing better on road, since this allows the asphalt mix to withstand high stress before failure.

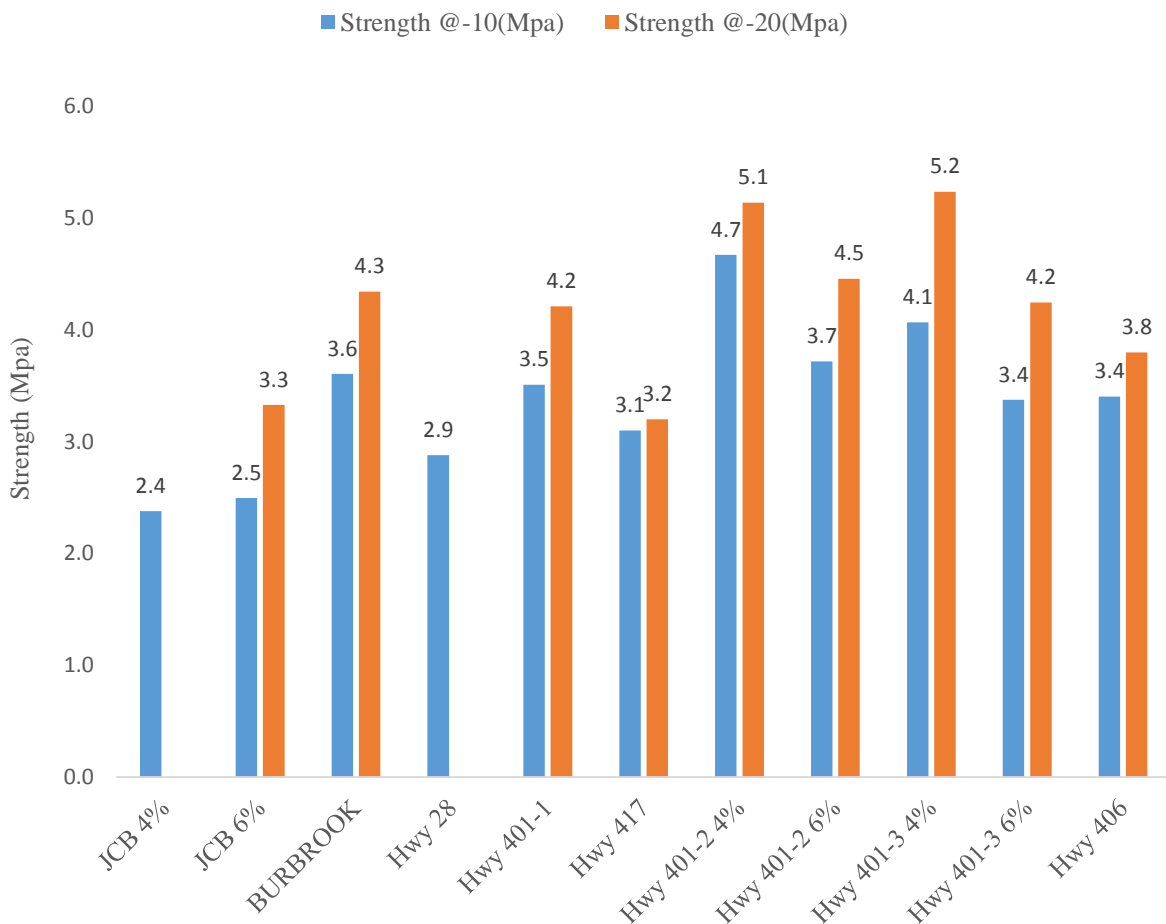


Figure 4.7: Strength values @ -10 and -20 for tested samples.

The highest tensile strengths were obtained for 401-1, 401-2, 401-3, BB and 406 samples, which were also some of the least compliant. The lowest strengths were obtained for both JCB samples, which also had some of the highest creep compliances. As expected, the strength increased when testing was performed at -20°C instead of -10°C after three hours of aging. The failure was also very brittle, resulting in complete failure of the sample, whereas at -10°C only a thin crack appeared across the face of the sample.

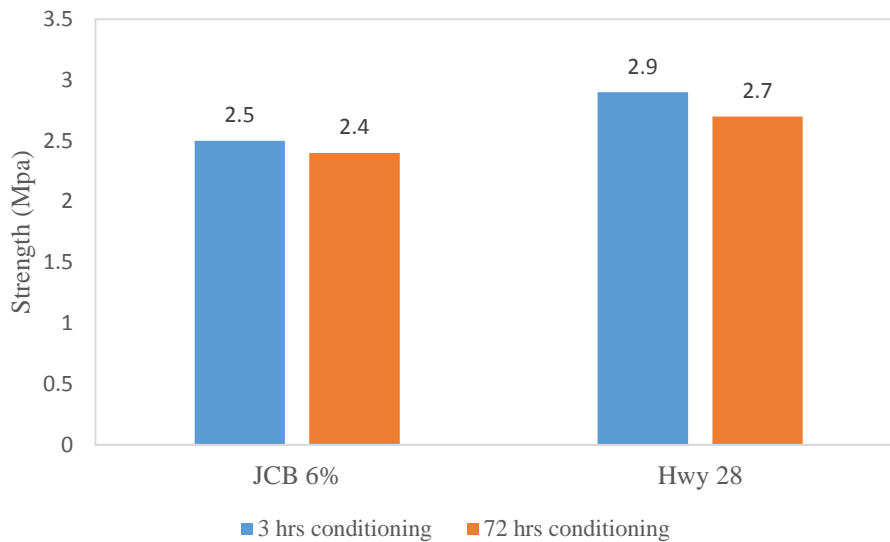


Figure 4.8: Tensile strength for Hwy 28 and JCB after 3 and 72 h conditioning.

Figure 4.8 shows the decrease in strength when additional aging for 72 h at -10°C is performed. This can again be probably explained by micro crack formation leading to sample damage. The CoV for the tensile strengths ranged from 2-5%, below the average 7% reported by other laboratories [79].

4.1.1 AASHTO MEPDG Software Results

The creep compliance and tensile data were used to obtain the predicted lifetime of the asphalt samples using the AASHTO MEPDG software. Failure is defined as 190 m of transverse cracking per km of road. A summary of the cracking results for the samples tested is shown in Table 4.1.

Table 4.1: Summary of MEPDG thermal cracking results

Sample	Aging	Cracking after 15 years (m/km)	Time to failure (years)
401-1	3 h	547	1
401-2- 4% voids	3 h	544.2	1
401-2- 6% voids	3 h	507.7	1
401-3- 4% voids	3 h	74.2	>15
417	3 h	398	2
28	3 h	285	5
28	72 h	322	3
406	3 h	50	>15
BB	3 h	162	>15
JCB – 4% voids	3 h	70	>15
JCB – 4% voids	72 h	432	9
JCB – 6% voids	3 h	102	>15
JCB – 6% voids	72 h	90	>15
401-3- 6% voids	3h	50.3	>15

Figure 4.9 shows an example of the thermal cracking output from the MEPDG software for all the tested samples. Six samples passed the test out of eleven tested. Passed samples include JCB (4 & 6 % air voids), BB, 401-3(4 & 6% air voids) and 406. The results also indicate that after 72 h of aging, the cracking after 15 years usually increases. However, in the case of JCB at 6% air voids, the opposite was found. This is likely due to damage from additional low temperature aging. This would increase the creep compliance, making the sample seem softer and better able

to relax and reduce stress accumulated from low temperature operation. In reality, the damage would likely decrease the time to failure of the asphalt sample, leading to similar results as JCB at 4% and Hwy 28 samples.

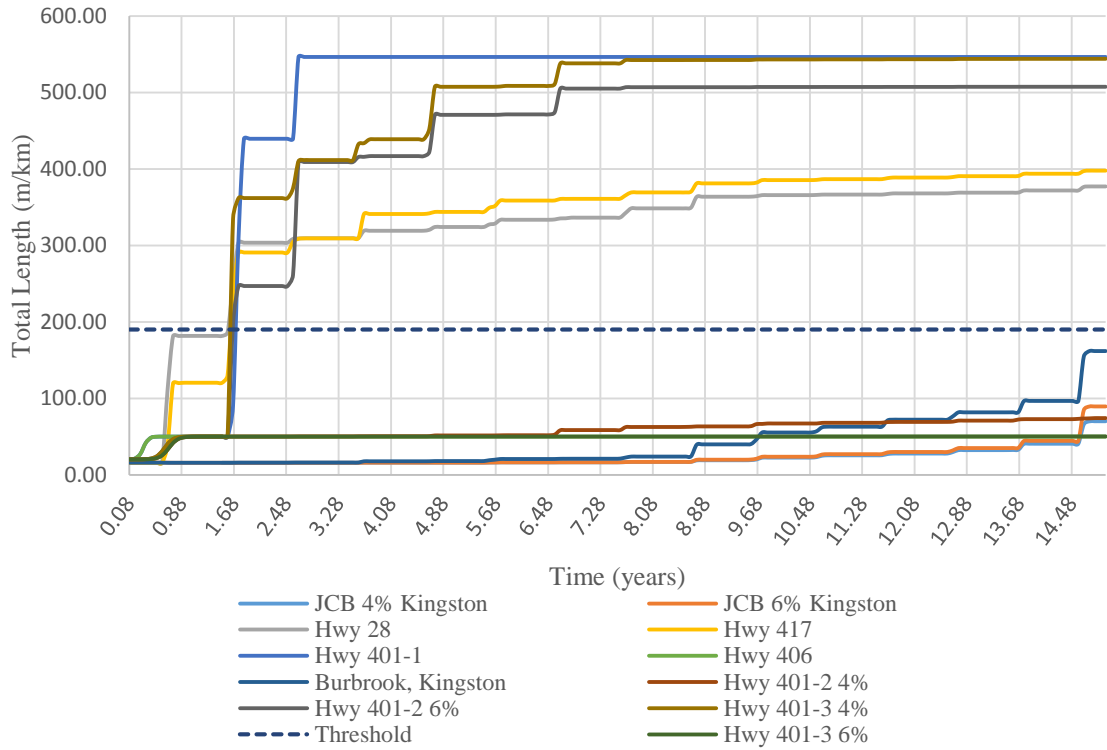


Figure 4.9: MEPDG results showing total length of thermal cracking for tested samples over time.

4.2 Dynamic Shear Rheometer Analysis

4.2.1 High Temperature Superpave Grading

The high temperature Superpave performance grades were determined for all recovered asphalt according to the standard procedures in the Dynamic Shear Rheometer (DSR) test. The high temperature Superpave grades measures the rutting resistance of asphalt pavement at higher temperature. The limiting temperatures for all recovered asphalt are summarized in Figure 4.10. The limiting temperature for 401-1 is found to be high, it might be due to over ageing in different processes (long time storage at high temperature, long time ageing during mixing, recovery at high temperature) and using RAP.

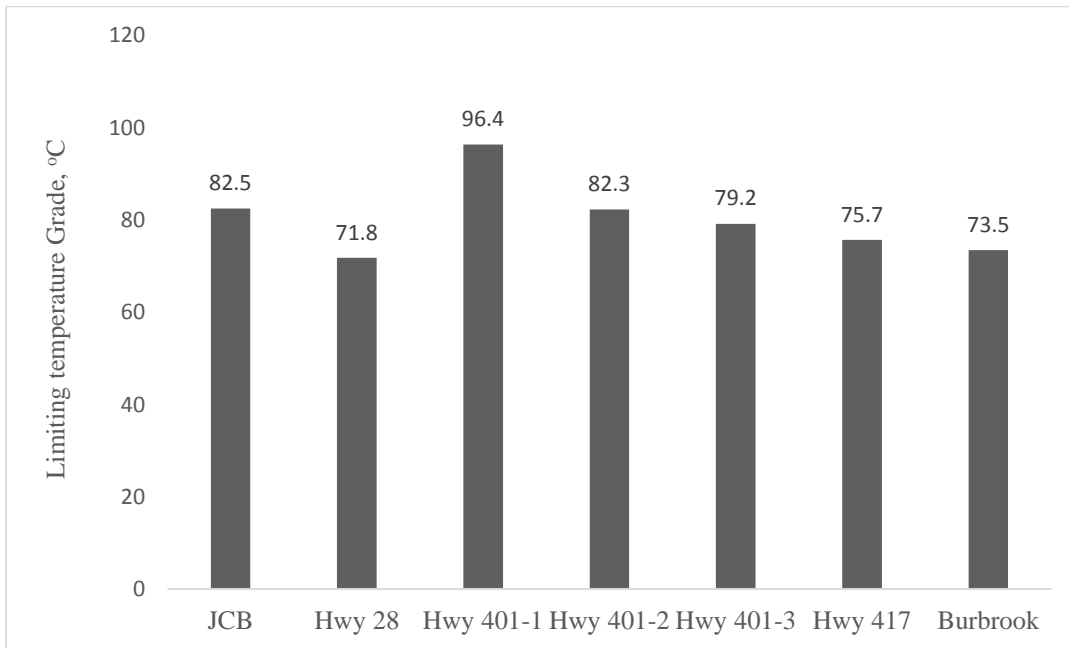


Figure 4.10: Limiting high temperature grades of recovered asphalts.

4.2.2 Intermediate Temperature Superpave Grading

The intermediate grades were determined for the recovered asphalt according to standard protocols using the DSR. According to the AASHTO M320 specification, the intermediate temperature PG grade is determined by the temperature at which $G^*\sin\delta$ is less than 5,000 kPa for a recovered asphalt [9]. Figure 4.11 shows the intermediate temperature performance grades for all the recovered samples.

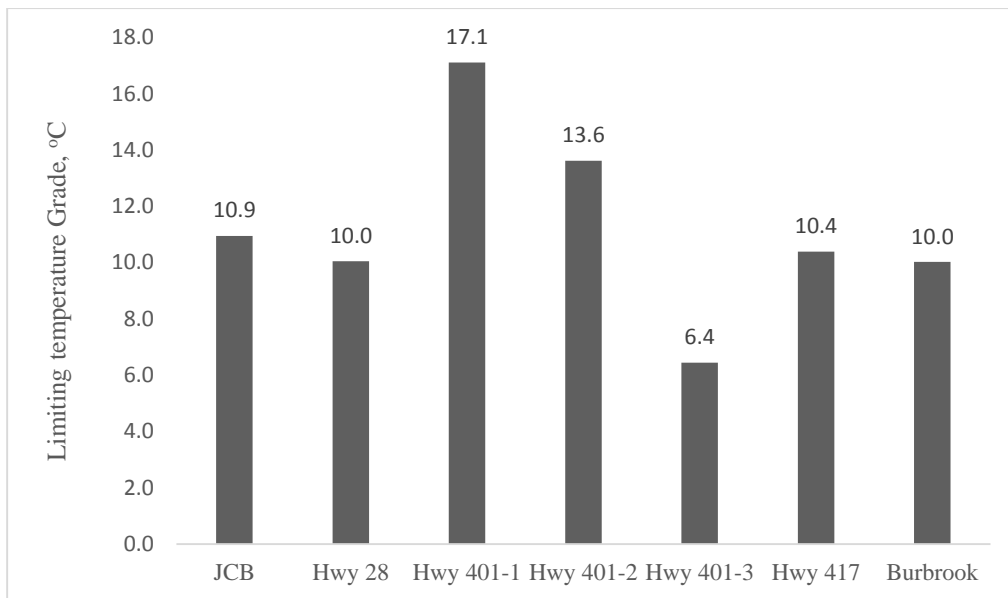


Figure 4.11: Limiting temperature of intermediate temperature grade of recovered asphalt.

The intermediate Superpave[®] grades provide a measure of resistance to fatigue cracking for asphalt binders. From the results it can be observed that recovered asphalt from 401-3 has the least intermediate temperature grade which implies that it is least susceptible to fatigue cracking as compared to the other modified binders. However, it must be noted that the intermediate Superpave[®] grades do not accurately correlate with fatigue cracking distress as compared to the

DENT test where the CTOD is able to accurately measure fatigue cracking resistance of the asphalt binders since it has a high correlation with fatigue cracking.

4.2.3 Black Space Diagrams

A Black space diagram is a graphical representation that can be used to characterize the rheological properties of asphalt binders. DSR test is performed for the study of the rheological properties of asphalt binder. Rheology is the branch of polymer science where the deformation and flow of materials is studied. The Black space diagram is able to distinguish between a single phase asphalt binder with a homogenous composition and a multiple phase asphalt binder with a heterogeneous composition. Asphalt binders with a single phase system are referred to as rheologically simple binders whereas asphalt binders which have two or more phase systems are referred to as rheologically complex binders. Black space diagrams are used to determine whether an asphalt binder is rheologically simple or complex. A Black space diagram in which there is a smooth progression of curves at different temperatures without any anomalous behaviour is called rheologically simple. In contrast, a rheologically complex binder would show a discontinuity in the progression of curves at different temperatures. This implies that the asphalt binder would have a phase separation or is undergoing some type of damage. Rheologically simple binders are easily predicted since their behavior is typical of a conventional viscoelastic material [8]. On the other hand, rheologically complex binders are difficult to predict in that their behavior does not follow that of a conventional viscoelastic material [8]. The figures below display the Black space diagrams at both high and low temperatures of the recovered asphalt binders.

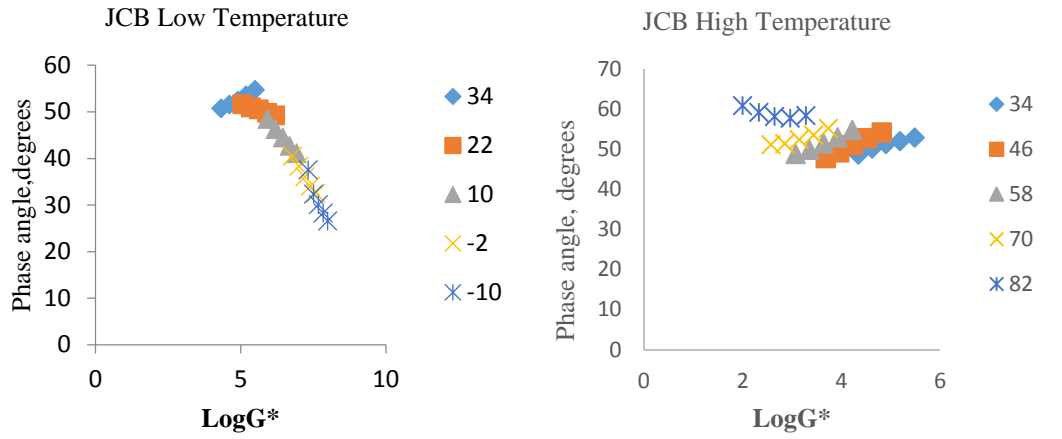


Figure 4.12 (a): Black space diagram for JCB at high and low temperature.

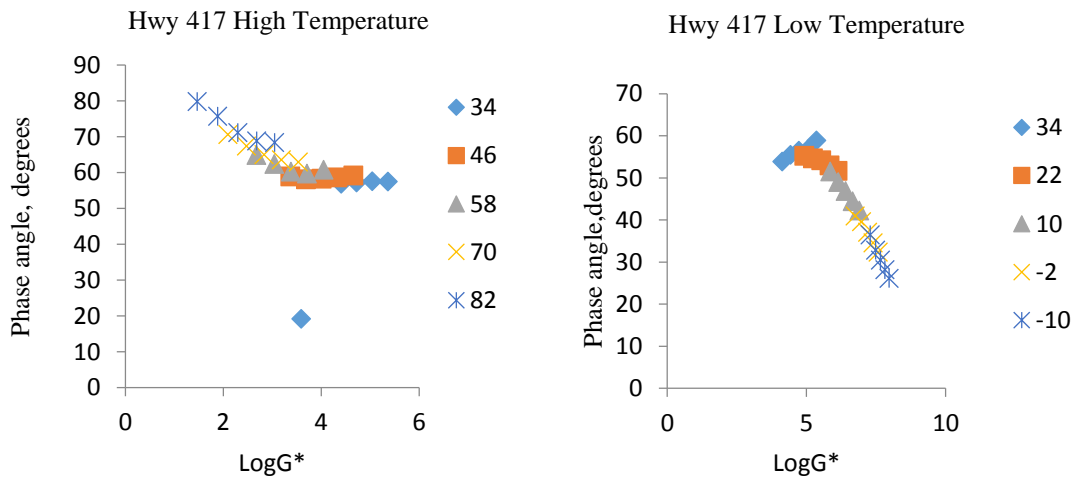


Figure 4.12 (b): Black space diagram for Hwy 417 at high and low temperature.

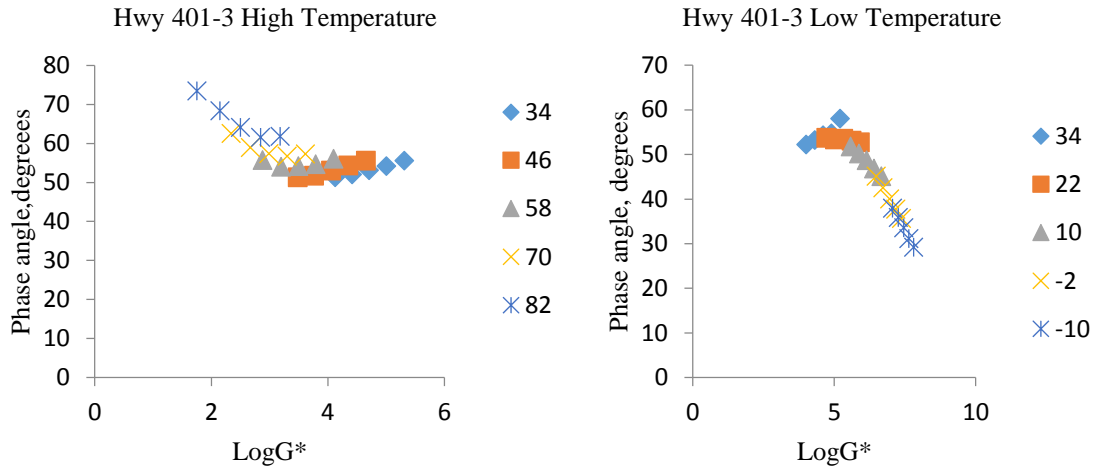


Figure 4.12 (c): Black space diagram for Hwy 401-3 at high and low temperature.

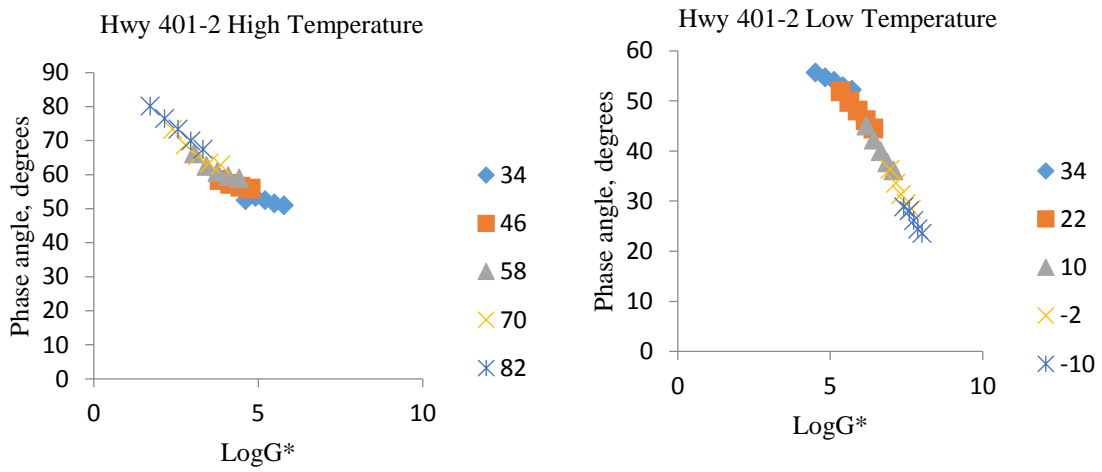


Figure 4.12 (d): Black space diagram for Hwy 401-2 at high and low temperature.

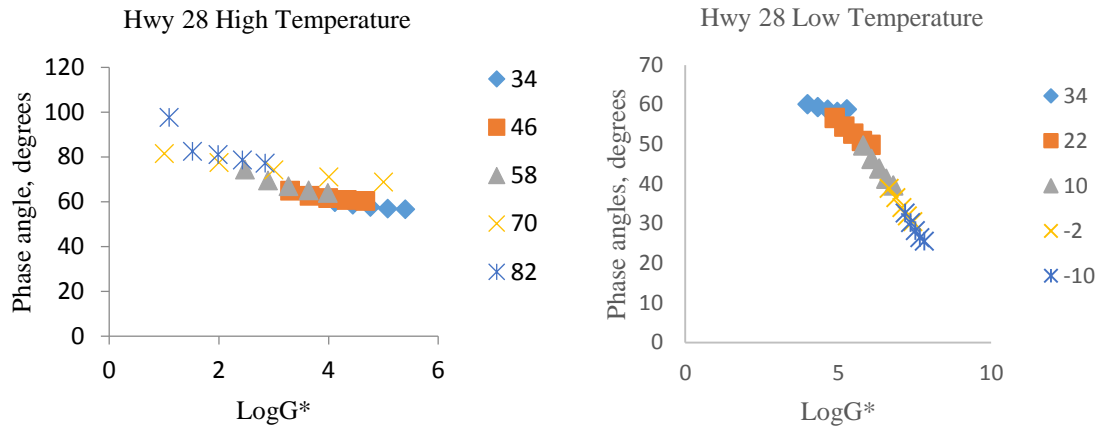


Figure 4.12 (e): Black space diagram for Hwy 28 at high and low temperature.

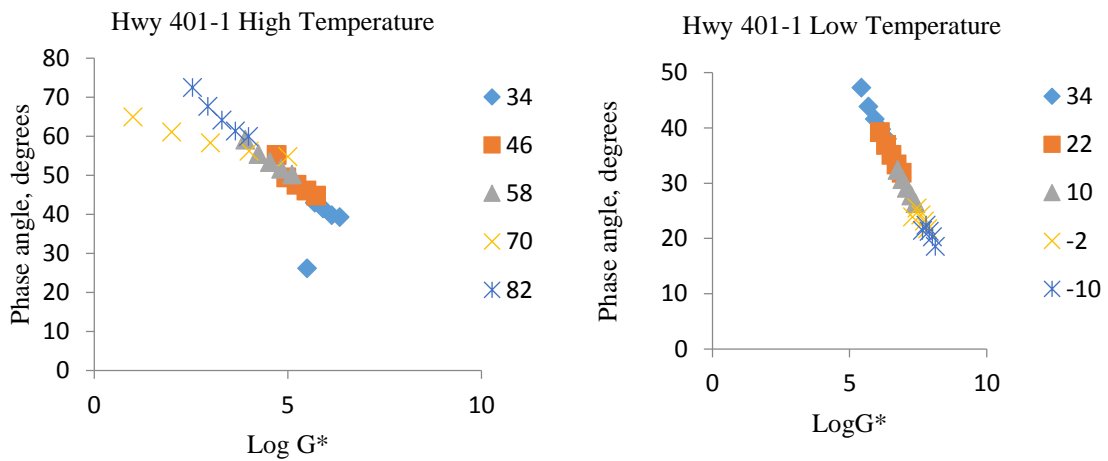


Figure 4.12 (f): Black space diagram for Hwy 401-1 at high and low temperature.

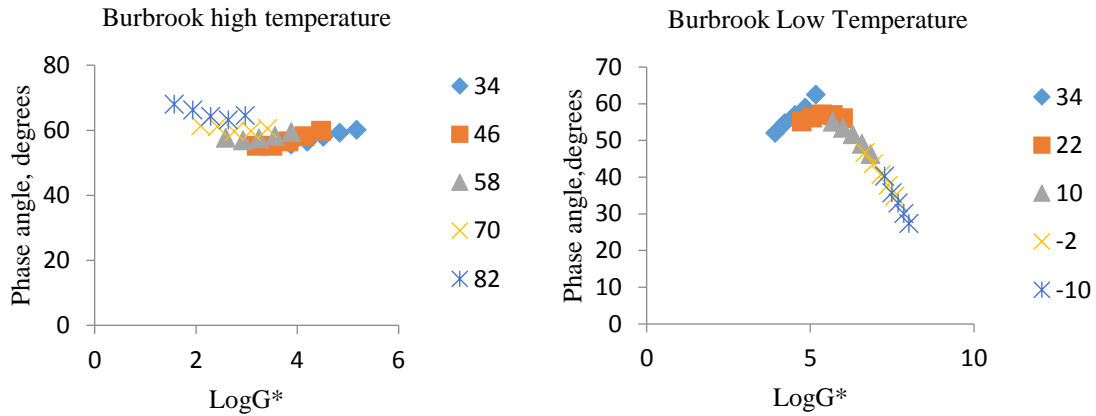


Figure 4.12 (g): Black space diagram for Burbrook road sample at high and low temperature.

By observing black space diagram for all the recovered binders it is seen that 401-1 and JCB samples show rheologically simple behavior at low temperature but deviated from rheologically simple behavior at high temperature. This might be due to phase separation at higher temperature.

4.3 Regular BBR Analysis

The regular BBR grades for the modified asphalt samples were determined according to AASHTO M320 standard test method. The test was carried out by conditioning the asphalt beams at -30°C , -20°C , -10°C and 0°C prior to testing at these temperatures. The creep stiffness ($S(t)$) and slope of the creep stiffness master curve ($m(t)$ -value) were determined using three point bending.

4.3.1 Low Temperature Grades

According to the AASHTO M320 specification, the low temperature PG grades are decided based on the limiting temperature where stiffness = 300 MPa or m -value = 0.300 for the PAV residue and the warmest of these two temperatures is used as a minimum performance grade temperature

of the asphalt binder [25]. A higher m-value indicates that the asphalt binder creeps at a faster rate to reduce the thermal stress and this is ideal to reduce low temperature cracking [80]. The results are summarized in Figure 4.10.

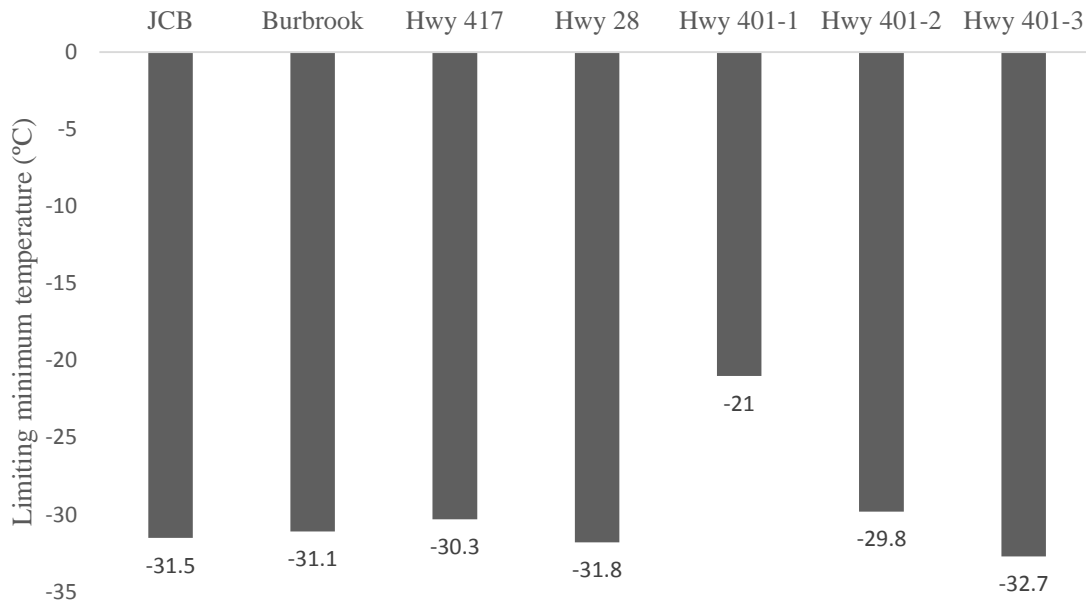


Figure 4.13: Low temperature grades of recovered binders.

As shown in Figure 4.13, some samples show grade deficit and others show excess. JCB, Burbrook, 401-2 show grade excess and rest show grade deficit. Grade deficit of recovered binders from 401-1, 401-3, 417 and 28 is likely due to the presence of oxidized asphalt molecules and heavy elements like Zn and Mo. Some binders which show grade excess may be due to polymer modification.

4.4 Extended BBR Analysis

LS-308 conditions at +10°C and +20°C above the actual grade temperature (i.e. pavement design temperature) for periods of 1 h and 72 h to simulate the effect of extended exposure to two different cold temperatures [69]. Exact grades of pass and fail temperatures are determined according to AASHTO M320 criteria by interpolation which involves plotting the grade on a semi-logarithmic scale [70].

4.4.1 Low Temperature Grades

The asphalt binders were conditioned for 1 and 72 h at -10°C. The limiting temperatures where $m(60) = 0.3$ and $S(60) = 300$ MPa were determined according to AASHTO M320 standard protocol and the warmest temperature among the two limiting temperatures gave the minimum performance grade temperature. The grade losses were then also determined to measure the durability of the binders. The following figure displays the low temperature grades according to Ontario's extended BBR protocol [69].

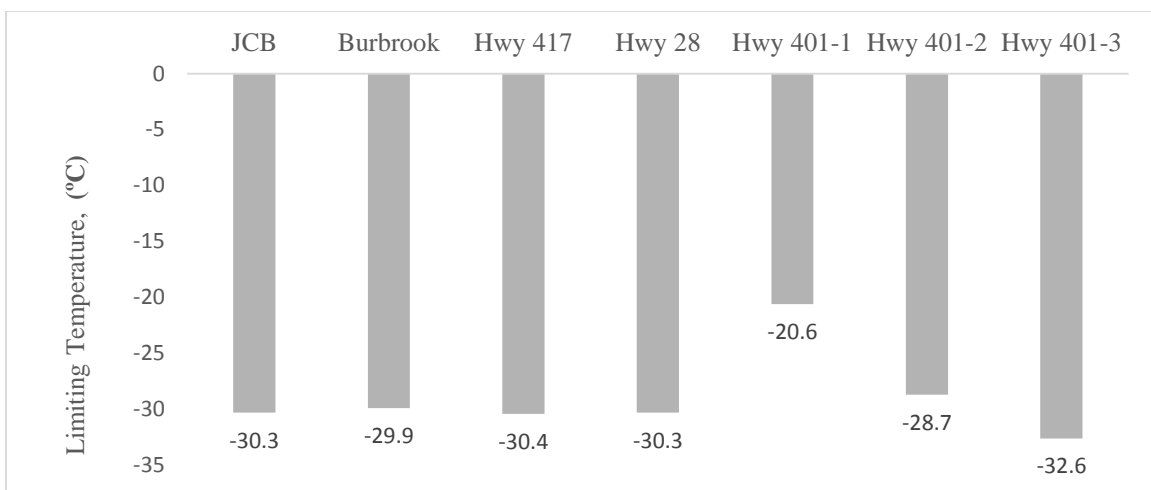


Figure 4.14: Low temperature grades of recovered binders extended BBR.

As shown in Figure 4.14, the limiting temperature for extended BBR is not much different from regular BBR it might be due to the recovered binders which are not PAV aged. Binders recovered from Kingston sample show some grade excess. Summary of binders grade deficit/excess conditioned for 72 h at -10°C is shown in Table 4.2.

Table 4.2: BBR summary of recovered binders.

Contract	Specification	PG	AASHTO M320 Grade, °C		Deficit/Excess, °C
			1h conditioning	72 h @ -10°C + 1 h	72 h
Hwy 401-1	MTO	70-28	-21	-20.6	7.4
Hwy 401-2	MTO	64-28 D	-29.8	-28.7	-0.7
Hwy 401-3	MTO	64-34	-32.7	-32.6	1.4
Hwy 417	MTO	64-34	-30.3	-30.4	3.6
Hwy 28	MTO	58-34 P	-31.8	-30.3	3.7
JCB	Kingston	64-28 XD	-31.5	-30.3	-2.3
BB	Kingston	58-28 XD	-31.1	-29.9	- 1.9

4.5 Double Edge Notched Tension (DENT) Testing

In order to have a better understanding of the ductile properties of asphalt binders, the essential work of fracture, EWF, concept was used to determine the strain tolerance and the failure characteristics of asphalt cements using the DENT test [81]. The DENT method has been

successfully used to classify asphalt binders with respect to their performance and also to distinguish superior quality binders from poor quality binders. In this test, the same ductility testing was carried out for all asphalt binders by stretching them at a constant rate of 50 mm/min in an isothermal water bath at 15°C until fracture occurred, as per the Ministry of Transportation of Ontario LS-299 standard testing procedure [71]. Figure 4.15 (a) and (b) shows the raw force-displacement trace for duplicate DENT tests on Burbrook recovered binder and Hwy 401-1 at 50 mm/min and 15°C.

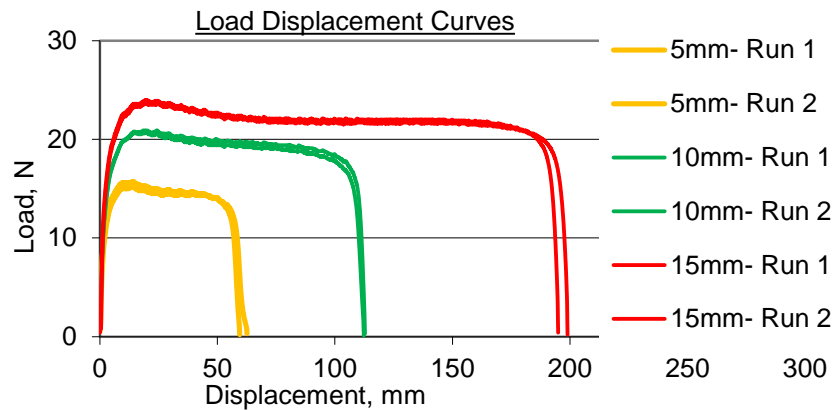


Figure 4.15 (a): Representative Force-Displacement Data for the DENT Test for Burbrook.

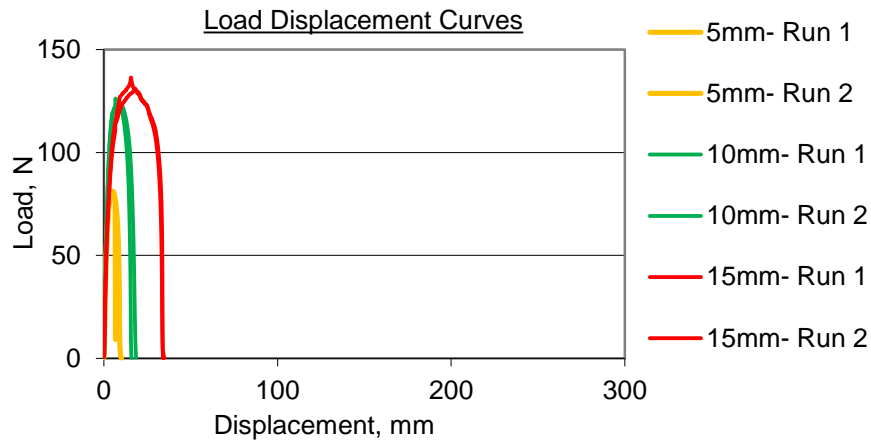


Figure 4.15 (b): Representative Force-Displacement Data for the DENT Test for Hwy 401-1.

4.5.1 Essential Works of Failure (W_e)

The essential work of failure is a material property since it is independent to the geometry of the asphalt cement sample. The EWF model is mostly used to determine the resistance of the fatigue cracking in asphalt cement pavement. The EWF model concept is best applied when the values of the essential work of fracture and the plastic work of fracture are relatively high in that cracking in the pavement occurs only when the strain tolerance of the pavement is exceeded [15]. However, it is assumed that high values of essential work of failure and plastic work of fracture are good for resistance to fatigue cracking [8].

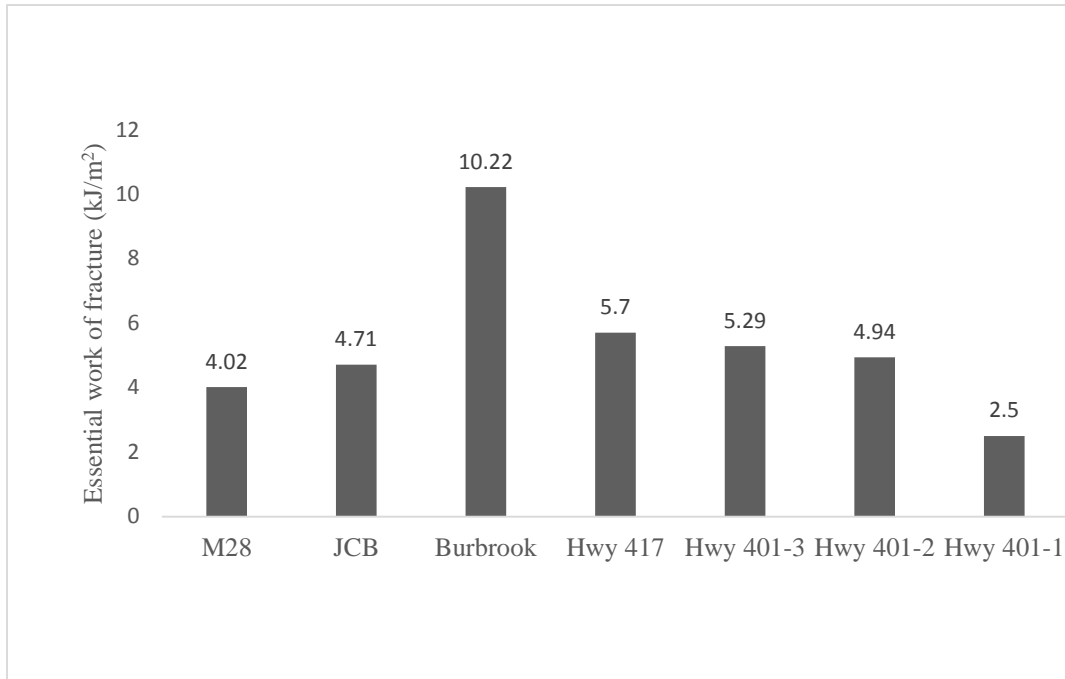


Figure 4.16: Essential work of fracture for recovered binders from different contracts.

It can be observed that the specific essential work of fracture is high for recovered binder from Burbrook road indicating that it has high strain tolerance to resist fatigue cracking. The remaining recovered samples with low values of essential work of fracture indicate that they have low strain tolerance and they could exhibit poor performance in service.

4.5.2 Plastic Work of Failure (βw_p)

The energy responsible for the non-essential or plastic deformation outside the fracture zone is the plastic work of failure. The shape of the plastic zone, which is the β factor, describes where the non-essential work is dissipated. The β factor can have different values depending on the geometry of the plastic zone. However, the β factor is not of primary importance since it is non-essential. The essential work of failure and the CTOD are rather of more interest. A high plastic work of

fracture usually occurs in an asphalt mixture when the asphalt binder is high, which in turn makes it less susceptible to fatigue cracking.

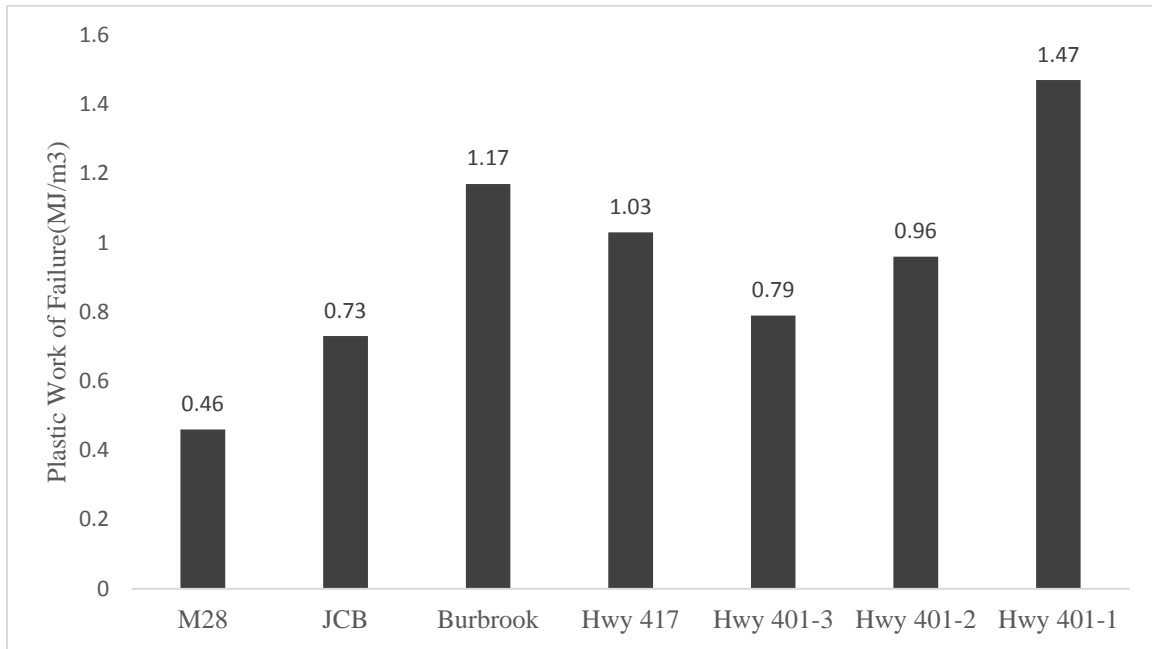


Figure 4.17: Plastic work of failure for recovered binders from different contracts.

Hwy 401 Central and Burbrook have higher plastic works of failure (β_{w_p}) as compared to the other modified asphalt binders as shown in the Figure 4.17. These samples exhibit a high strain tolerance. The remaining samples exhibited relatively low values of plastic works of failure (β_{w_p}).

4.5.3 Approximate Critical Crack Tip Opening Displacements

The CTOD parameter provides a measure of strain tolerance in the ductile state under conditions of severe confinement. CTOD explains how the propagation of cracking occurs under ductile conditions during periods of increased loading and strain in the asphalt pavement [82]. Although

the essential work of failure and the plastic work of fracture are able to predict fatigue cracking in the asphalt pavement, the correlation existing between the CTOD and the fatigue properties are higher comparatively due to its high accuracy when predicting fatigue cracking and ductile fracture properties of both binders and mixtures [82]. It has been proved that this parameter “shows promise for performance grading of both binders and mixtures for fatigue cracking at temperatures and rates of loading that cover the ductile regime” [83]. Figure 4.18 shows the CTOD values obtained per sample.

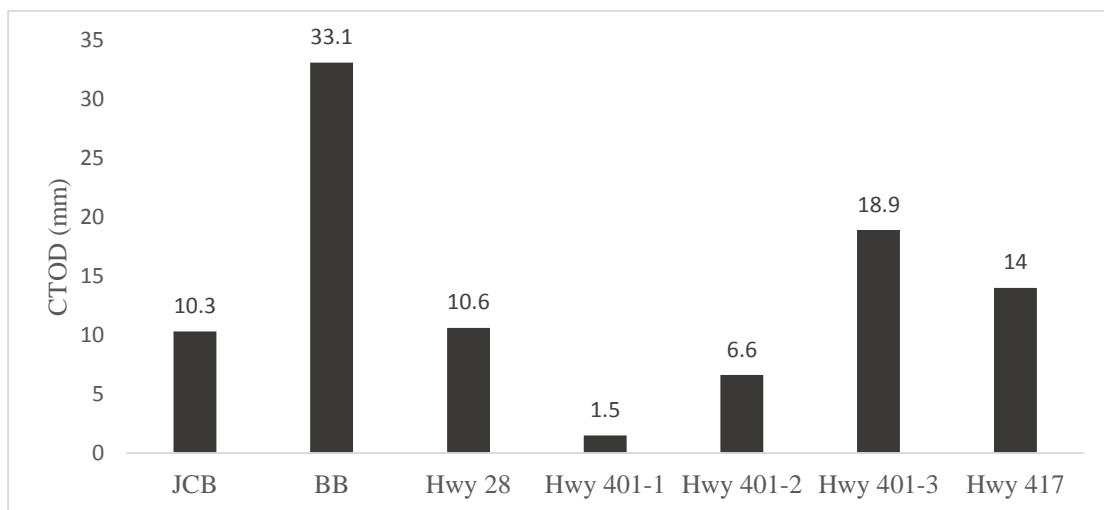


Figure 4.18: CTOD values for all recovered binders.

It can be observed that recovered binder from HWY 401-1 has very low CTOD that means it has very low strain tolerance in the ductile state, thus it is more susceptible to premature cracking in service comparatively. However, recovered binder from Burbrook road which has higher CTOD values have a better resistance to fatigue cracking.

4.6 XRF and FTIR Analysis of Recovered Asphalt

The asphalt cement was recovered from all samples and analysed using XRF. Peaks at 8.64 and 17.48 keV were noticed in selected binders, corresponding to zinc and molybdenum. These peaks were normalized to those obtained from a waste engine oil sample acquired from a Western supplier. The relative amounts are summarized in Table 4.3 and Figure 4.19.

Table 4.3: Relative zinc and molybdenum counts obtained from XRF analysis

Sample	Relative Zinc Count (%)	Relative Molybdenum Count (%)
401-1	1.80	0.70
401-2	5.63	6.40
401-3	1.41	3.94
417	0.81	2.20
28	8.22	5.37
BB	0.66	1.06
JCB	0.60	1.23

High amounts of zinc and molybdenum were found in 401-1, 401-2, 401-3, and 28 samples. The presence of these metals might be explained by the addition of waste engine oils to the asphalts [84] as they are often used in anti-wear additives. The use of waste engine oils in asphalt leads to physical hardening and an overall decrease in pavement performance [84]. This may explain the poor performance for the 28 sample.

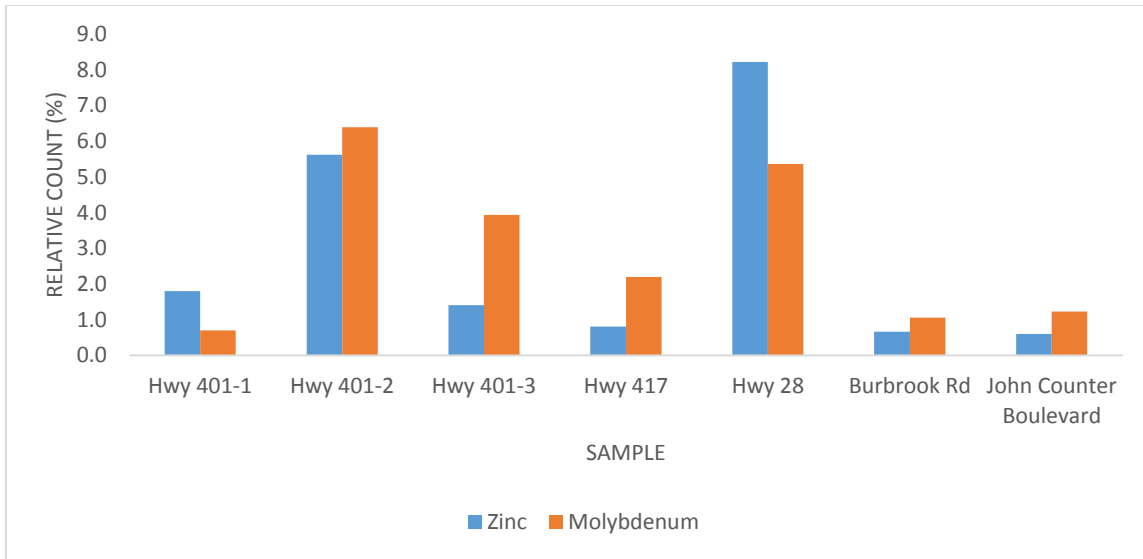


Figure 4.19: Zinc and molybdenum content of all samples, relative to Newalta waste engine oil residue sample.

FTIR was also performed on the recovered asphalt to look for the presence of polymer addition. Polymer modified binders perform better than unmodified binders, leading to better thermal performance among other advantages [85]. A common polymer modifier is styrene butadiene styrene (SBS), so styrene and butadiene peaks were identified and the areas were normalized to the CH stretch peak area. The carbonyl peak was also of interest as it indicates oxidized residues in the asphalt cement, which leads to oxidative hardening and decreased pavement performance [86]. The relative amounts of carbonyl, styrene, and butadiene are summarized in Table 4.4 and Figure 4.20.

Table 4.4: Relative amounts of carbonyl, butadiene, and styrene obtained from FTIR analysis

Sample	Relative Carbonyl Content (%)	Relative Butadiene Content (%)	Relative Styrene Content (%)
401-1	1.14	0.03	0.02
401-2	0.75	0.07	0.08
401-3	0.41	0.12	0.11
417	0.38	0.13	0.12
28	0.84	0.07	0.10
BB	0.09	0.13	0.11
JCB	0.57	0.12	0.12

Table 4.4 shows, the 401-1, 401-2, and 28 samples had a very high carbonyl content, meaning these could have contained oxidized residues at the time of testing. This premature oxidation may be responsible for their poor predicted lifespans. BB had low carbonyl content, and both BB and JCB had high relative styrene and butadiene content. This high polymer content is responsible for good pavement performance obtained from the MEPDG software for these samples. Interestingly, even though the 417 sample had low carbonyl content, high polymer content, and little evidence of large amounts of waste engine oil addition, it still did not perform as well as the Kingston samples. This seems to indicate that other factors affect the low temperature performance of the asphalt mixtures.

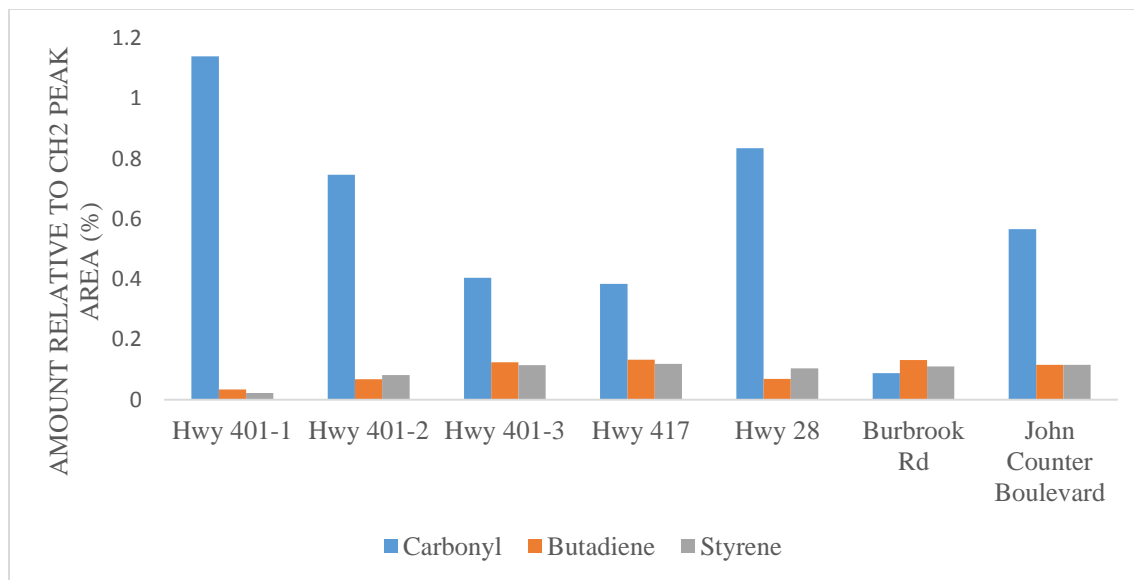


Figure 4.20: Carbonyl, butadiene, and styrene content of all samples, normalized to CH stretch peak area.

Chapter 5

Summary, Conclusion and Recommendation

- (1) In all cases the creep compliance remains almost constant at -20 and -30 since asphalt behaves almost brittle at very low temperature. In one case creep compliance is increased at additional low temperature physical hardening/aging and in all cases the decrease in tensile strength for asphalt mixtures is found. This looks to indicate that the samples are being damaged, likely due to the difference in coefficients of thermal expansion between the aggregate and the asphalt cement. This difference could cause the asphalt cement pulling away from the aggregate, causing microcrack formation within the structure. In the case of creep compliance, the softening of the sample actually led to an improvement in the predicted performance. However, if the sample is damaged, it would likely result in a poorer actual performance.
- (2) Generally, it was observed that samples with a high creep compliance had a low tensile strength and vice-versa. However, the Hwy 401-3 sample had the highest creep compliance while still having a relatively high tensile strength. A high creep compliance is required, since this allows good relaxation which decreases stress accumulated in the asphalt. In addition, a high tensile strength is preferred since this make sure the asphalt can resist large stresses before cracking.
- (3) The predicted cracking times of the samples designed using the City of Kingston standards (BB and JCB) outperformed most of the samples designed using MTO standards by a significant amount.

- (4) XRF analysis of the recovered asphalt cement showed evidence of addition of waste engine oil to the MTO Hwy 401-1, Hwy 401-2, Hwy 401-3 and Hwy 28 samples. Kingston samples contain very low counts of zinc and molybdenum that reflects the absence or very low contents of waste engine oil.
- (5) FTIR analysis showed the likely evidence of oxidized residues in the Hwy 401-1, Hwy 401-2 and Hwy 28 samples. The analysis also showed low amounts of polymer modification in the Hwy 401-1, Hwy 401-2 and Hwy 28 samples.
- (6) Most of the samples designed according to MTO specifications had evidence of waste engine oil addition and/or large amounts of oxidized residues and low polymer modification. These samples also resulted in low predicted lifetimes. However, the sample from Hwy 417 did not show evidence of waste engine oil addition or oxidized residues and contain comparatively high polymer modification but still had a short predicted lifetime. This indicates other factors besides the factors above explained are also responsible for predicted performance.

Recommendations

- (1) Reproducibility of AASHTO pavement software should be improved.
- (2) For better performance of road the addition of waste engine oil to asphalt binder should be prevented.
- (3) Polymer modification of asphalt binder should be done.
- (4) Monitor the road performance of JCB and BB over the next few years to see if they are in fact much better than the MTO contracts. If so, implement the City of Kingston specifications as soon as possible.

References

- [1] Herbert, A., *Asphalts and Allied Substances: Their Occurrence, Modes of Production, Uses in the Arts, and Methods of Testing* " **1938**.
- [2] Sorensen, A., Wichert, B. *Asphalt and Bitumen* in Ullmann's Encyclopedia of Industrial Chemistry Wiley-VCH, Weinheim," **2009**.
- [3] Brule, B., *Polymer Modified Asphalt Cement Used in Road Construction Industry: Basic Principles in Asphalt Science and Technology*; Usmani, A.M., Ed ; New York, Basel, Hong Kong," **1997**.
- [4] Croney, P., Croney, D., *Design and Performance of Road Pavements*, New York ,3rd edition: McGraw-Hill, **1997**.
- [5] Pavement Interactive;
<http://www.pavementinteractive.org/article/hma-pavement/> Accessed: August **2014**.
- [6] Meyer, R. F., De Witt, W., U. S. Geo. Sur. Bull., 14, **1991**.
- [7] Mullins, O., and Sheu, E., (Editors). *Structure & Dynamics of Asphaltenes*, 1st Edition. Springer, 1-17, **1999**.
- [8] Agbovi, K.H., *Effect of Low temperatures, repetitive stresses and chemical aging on thermal and fatigue cracking in asphalt cement pavement on high 417*, M.Sc. Thesis, Department of Chemistry, Queen's University, Kingston, Canada, **2012**
- [9] *Superpave: Performance Graded Asphalt Specification and Testing* New York, Asphalt Institute, **2003**.
- (10) Read, J., Whiteoak, D., In the Shell Bitumen Handbook, Fifth edition; Hunter, R. N., Ed.; Thomas Telford: London, **2003**.
- (11) *The Asphalt Handbook; 7th Edition*, Ed.; Asphalt Institute: USA, **2007**.

- [12] Kriz, P., Stastna, J., Zanzotto, L., *Temperature Dependence and Thermo-reversibility of Physical Hardening of Asphalt Binders*, submitted to 4th Eurasphalt & Eurobitume Congress, Copenhagen, Denmark, May 21-23, **2008**.
- [13] Baglieria, O., Dalmazzoa, D., Baraziaa, M., Tabatabaeeb, H.A., Bahiab, H.U., *Influence of Physical Hardening on the Low-Temperature Properties of Bitumen And Asphalt Mixtures* Department of Environmental, Land and Infrastructure Engineering, Politecnico di Torino, 24 Corso Duca degli Abruzzi, Torino 10129, Italy.
- [14] Adhikari, T.N., *Quality And Durability Of Rubberized Asphalt Cement and Warm Rubberized Asphalt Cement* M.Sc. Thesis, Department of Chemistry, Queen's University, Kingston, Canada, **2013**.
- [15] Paul, S.S.K., *Effects Of Warm Mix Additives And Dispersants On Rheological, Aging And Failure Properties Of Asphalt Cements* M.Sc. Thesis, Department of Chemistry, Queen's University, Kingston, Canada, **2013**.
- [16] Lu, X., Isacson, U., *Effect of ageing on bitumen chemistry and rheology*, Construction and Building materials, 15-22, 16, **2002**.
- [17] Petersen, J.C., *Chemical composition of asphalt as related to asphalt durability: state of the art*. Transport. Res. Record, 13-30, 999, **1984**.
- [18] Traxler, R.N., Coombs, C.E., *Proceedings of the Fortieth Annual Meeting, American Society for Testing Materials*, New York City, NY, 549, 37(II), **1937**.
- [19] Struik, L.C.E., *Physical Aging in Amorphous Polymers and other Material*, Elsevier Scientific Publishing Co. Amsterdam, **1978**.
- [20] Anderson, D.A., Bahia, H.U., Dongre, R., Sharma, M.G., Antle, C.E., Button, J. *physical characterization*, 369, 3, **1994**.

- [21] Bahia, H.U., Anderson DA. *Glass transition behaviour and physical hardening of asphalt binders*. J Assoc Asphalt Paving Technol, 93-129, 62, **1993**
- [22] Brown, A.B., Sparks, J.W., Smith, F.M., *Steric hardening of asphalts*. Proc Assoc Asphalt Paving Technol, 486-94, 26, **1957**
- [23] Pavement Interactive:
<http://www.pavementinteractive.org/article/mix-designsuperpave-method/> Accessed:
 August **2008**.
- [24] Mix design: [http://www.in.gov/indot/files/Chapter_04\(4\).pdf](http://www.in.gov/indot/files/Chapter_04(4).pdf)
- [25] Kanbar, N., *Comparison Of Ethylene Terpolymer, Styrene butadiene, And Polyphosphoric Acid Type Modifiers For Asphalt Cement*, M.Sc. Thesis, Department of Chemistry, Queen's University, Kingston, Canada, **2012**.
- [26] http://classes.engr.oregonstate.edu/cce/spring2014/ce492/Modules/09_pavement_evaluation/09-7_body.htm.
- [27] Henry, K.A., *Effects of Low Temperatures, Repetitive Stresses and Chemical Aging on Thermal and Fatigue Cracking in Asphalt Cement Pavements on Highway 417*. MSc. Thesis, Department of Chemistry, Queen's University, Kingston, Ontario, Canada, **2012**.
- [28] Pavement Interactive:
<http://www.pavementinteractive.org/article/general-guidancepavement-distress>,
 Accessed: August **2014**.
- [29] http://en.wikipedia.org/wiki/Crocodile_cracking.
- [30] Tao, X., Xiaoming, H., *Investigation into causes of in-place rutting in asphalt pavement*. Construction and Building Materials, 525–530, 28, **2012**.

- [31] Simpson, A.L., *Characterization of transverse profile*. Transport Res Rec, 185–91. 1655, **1999**.
- [32] Fontes, L.P.T.L., Triches, G., Pais, J.C., Pereira, P.A.A., *Evaluating permanent deformation in asphalt rubber mixtures*. Construction and Building Materials, 1193–1200, 24, **2010**
- [33] Soleimani, A., *Use of dynamic phase angle and complex modulus for the low temperature performance grading of asphalt cement*, M.Sc. Thesis, Department of Chemistry, Queen’s University, Kingston , Canada, **2009**
- [34] Huang, X.M., Zhang, Y.Q., *A new creep test method for asphalt mixtures*. Road Materials and Pavement design, 969–991, 11, **2010**.
- [35] Archilla AR. *Use of superpave gyratory compaction data for rutting prediction*. Journal of Transport Engineering, 734–741, 132, **2006**.
- [36] http://www.dot.state.mn.us/mnroad/projects/Low_Temp_Cracking/ Department of Transportation Minnesota.
- [37] Yee, P., Aida, B., Hesp, S.A.M., Marks, P., Tam, K.K., *Analysis of three premature low temperature pavement failures*. Journal of the Transportation Research Board, 44-51, **2006**.
- [38] Pavement Interactive:
<http://www.pavementinteractive.org/article/general-guidancepavement-distress>.
Accessed: August **2014**.
- [39] Road Science:
<http://www.roadscience.net/services/distress-guide/stripping-moisture-damage>.
Accessed: August **2014**.
- [40] Asphalt Institute, Superpave mix design, Superpave series-2, **2003**.

- [41] Zaniwski, J.P., Pumphery, M.E., *Evaluation of Performance Graded Asphalt Binder Equipment and Testing Protocol*, Department of Civil Engineering, Morgantown, West Virginia, **2004**.
- [42] Asphalt Institute, the Asphalt Handbook, U.S.A., MS 4, **1965**.
- [43] Mack C.J., *Colloid Chemistry of Asphalts*. Journal of Physical Chemistry, 2901, 36, **1932**.
- [44] John R., David W., The Shell bitumen hand book. Thomas Telford Services Limited, 352, **2010**.
- [45] Hussain U.B., Andrew H., Pouya T. *Effect of WMA Additives on Binders Workability and Performance*. 2nd International Warm Mix Asphalt Conference, St. Louis, Missouri, October 12, **2011**.
- [46] Xu, Q., Chen, H., Prozzi, J.A., *Performance of Fiber Reinforced Asphalt Concrete under Environmental Temperature and Water Effect*. Construction and Building Material, 2003-2010, 24, **2010**.
- [47] Bates, R., Worch, R., Engineering Brief No. 39, *Styrene-butadiene rubber latex modified asphalt*. Federal Aviation Administration, Washington, DC, **1987**.
- [48] Thompson DC. Hoiberg AJ, editor. Bituminous materials: *Asphalt tars and pitches*. Robert Krieger Publishing Co.; **1979**.
- [49] Adhesive and Glue:
<http://www.adhesiveandglue.com/elastomer.html>. Accessed: August, **2014**.
- [50] Yetkin, Y., *Polymer modified asphalt binders*, Construction and Building Materials, 66–72, 21, **2007**.
- [51] Baumgardner, G.L., *why and how of polyphosphoric acid modification*, Journal of Association of Asphalt Paving Technologists, 663-678, 79, **2010**.

- [52] Buncher, M., D'angelo J.A., *Polyphosphoric Acid Modification of Asphalt* Transportation Research Board Circular, 12, January **2012**.
- [53] Burk, R. E., Whitcare, C.H. *Asphalt from Petroleum Residue* US Patent 2, 208, 179, **1939**.
- [54] Kodrat, I., Dave, S., Hesp S.A.M. *Transportation Research Record: Journal of the Transportation Research Board*, 1998, 47, **2007**.
- [55] Bitumen and asphalt expert:
<http://www.bitumenengineering.com/modified-bituminousmaterials/polymer-modified-bitumen>, Accessed: August, **2014**.
- [56] Vassiliev, N.Y., Davison, R. R., Williamson, S.A., Glover, C. J., *Air Blowing of Supercritical Asphalt Fractions*, *Ind. Eng. Chem. Res.*, 1773-1780, 40, **2001**.
- [57] Poirier, M. A., Sawatzky, H., *Changes in Chemical Component Type Composition and Effect on Rheological Properties of Asphalts*. *Fuel Sci. Technol. Int.*, 681, 10, **1992**.
- [58] Pavement interactive:
<http://www.pavementinteractive.org/article/penetration-test/> Accessed: August **2014**.
- [59] ASTM, *Annual Book of ASTM Standards, Section 4, Construction, Volume 4.03 Road and Paving Materials*, American Society for Testing and Materials, Pennsylvania, **1998**.
- [60] *Laboratory-Pavement Materials; Penetration of Bituminous Materials*, *School of Civil and Structural Engineering*, Nanyang Technological University, **2002**.
- [61] American Society for Testing and Materials, *Standard Test Method for Softening Point of Bitumen (Ring and Ball method)*, ASTM, D36-95, **1995**.

- [62] Pavement Interactive:
<http://www.pavementinteractive.org/2012/10/02/what-is-mechanistic-empirical-design-the-mepdg-and-you/> Access: August **2014**.
- [63] Phillip Maurer, *Asphalt Performance Testing*, ENCH 417 Thesis Project, Queens University, Kingston, Canada, **2014**.
- [64] ARA, Inc., ERES Consultants Division, "Guide for Mechanistic Empirical Design of New and Rehabilitated Pavement Structures," National Cooperative Highway Research Program, Champaign, **2004**.
- [65] Richardson, D.N., Lusher, S.M., *Determination Of Creep Compliance And Tensile Strength of Hot Mix Asphalt For Wearing Courses in Missouri*, Missouri University of Science And Technology, April **2008**.
- [66] *Determining Creep Compliance and Strength of Hot Mix Asphalt Using Indirect Tensile Test Device*, AASHTO Designation T322-07.
- [67] Pavement Interactive:
<http://www.pavementinteractive.org/article/dynamic-shear-rheometer/> Accessed: August **2014**.
- [68] Mang, T., Bituminous materials, University of Florida.
<http://nersp.nerdc.ufl.edu/~tia/Bituminous-Materials.pdf>. Accessed: August **2014**.
- [69] Ministry of Transportation of Ontario; LS-308 – *Determination of Performance Grade of Physically Aged Asphalt Cement Using Extended Bending Beam Rheometer (BBR) Method*, Revision 24 to Laboratory Testing Manual, **2007**.

- [70] American Association of State Highway and Transportation Officials, Standard Specification for Performance-Graded Asphalt binder, Washington D.C., AASHTO M320, **2002**.
- [71] Ministry of Transportation of Ontario; LS-299 – *Determination of Asphalt Cement's Resistance to Ductile Failure Using Double-Edge-Notched Tension Test (DENT)*, Revision 24 to Laboratory Testing Manual, **2007**.
- [72] AASHTO T312 - Preparing and Determining Density of Hot Mix Asphalt (HMA) Specimens By Means Of the Superpave Gyrotory Compactor.
- [73] Bulk Specific Gravity of Compacted Hot Mix Asphalt Using Saturated Surface-Dry Specimens, in AASHTO T 166-07., American Association of State Highway and Transportation Officials, Washington, D.C., **2007**.
- [74] American Association of State Highway and Transportation Officials, "*Determining the Creep Compliance and Strength of Hot Mix Asphalt (HMA) Using the Indirect Tensile Test Device*," AASHTO, **2007**.
- [75] US Department of Transportation: Federal Highway Administration; "*Background of Superpave Asphalt Binder Test Methods*", Publication No. FHWA-SA-94-069, **1994**.
- [76] Asphalt Institute, "*Performance Graded Asphalt Binder Specification and Testing*", Superpave Series No. 1 (SP-1), 22-28, **2003**.
- [77] Ali, O. "*Evaluation of the Mechanistic Empirical Pavement Design Guide*," National Research Council Canada, **2005**.
- [78] Zofka, A., Mrasteanu, M. and Tuross, M., "*Investigation of Asphalt Mixture Creep Behavior Using Thin Beam Specimens*," in Multiscale and Functionally Graded Materials, **2006**.

- [79] Christensen, D. W. and Bonaquist, R. F. "*Evaluation of Indirect Tensile Test (IDT) Procedures for Low-Temperature Performance of Hot Mix Asphalt*," NCHRP, Washington, **2004**.
- [80] Superpave; Performance Graded Asphalt Specification and Testing, New York, Asphalt Institute, **2003**.
- [81] Jung, D. H., Vinson, T. S.; *Low-Temperature Cracking: Test Selection*. SHRP-A-400. Strategic Highway Research Program, National Research Council, Washington, D.C- **1994**.
- [82] Andriescu, A., Gibson, N., Hesp, S.A.M., Qi, X., Youtcheff, J.S.; *Validation of the Essential Work of Fracture Approach to Fatigue Grading of Asphalt Binders*. Journal of the Association of Asphalt Paving Technologists, 1-37, 75, **2006**.
- [83] Bodley, T., Andriescu, A., Hesp, S. A. M., Tam, K. K.; Journal of the Association of Asphalt Paving Technologists, 345, 76, **2007**.
- [84] Hesp, S.A.M., Shurvell, H. F., "*X-ray fluorescence detection of waste engine oil residue in asphalt and its effect on cracking in service*," International Journal of Pavement Engineering, 541-553, 11, **2010**.
- [85] Yldirim, Y., "Polymer Modified Asphalt Binders," *Construction and Building Materials*, 66-72, 21, **2005**.
- [86] Asphalt Institute, Performance Graded Asphalt Binder Specification and Testing Superpave Seris No. 1 (SP-1), Lexington: Asphalt Institute, **2003**.

